REPORT DOCUMENTATION PAGE

Form Approved
OMB No. 0704-0188

1. AGENCY USE ONLY (Leave blank)	2. REPORT DATE	3. REPORT TYPE AND DATES COVERED
		FINAL 1 Feb 93 - 31 Oct 94

4. TITLE AND SUBTITLE
HIGH ENERGY PULSED MICROWAVE SOURCES

5. FUNDING NUMBERS
61102F
2301/ES

6. AUTHOR(S)
Dr John A. Nation

AFOSR-TR-95-0232

7. PERFORMING ORGANIZATION NAME(S) AND ADDRESS(ES)
Cornell University
Ithaca, NY 14853

8. PERFORMING ORGANIZATION REPORT NUMBER

9. SPONSORING MONITORING AGENCY NAME(S) AND ADDRESS(ES)
AFOSR/NE
110 Duncan Avenue Suite B115
Bolling AFB DC 20332-0001

10. SPONSORING MONITORING AGENCY REPORT NUMBER
F49620-93-1-0103

11. SUPPLEMENTARY NOTES

12a. DISTRIBUTION AVAILABILITY STATEMENT
APPROVED FOR PUBLIC RELEASE: DISTRIBUTION UNLIMITED

12b. DISTRIBUTION CODE

13. ABSTRACT (Maximum 200 words)

SEE FINAL REPORT ABSTRACT

14. SUBJECT TERMS	15. NUMBER OF PAGES
	16. PRICE CODE

17. SECURITY CLASSIFICATION OF REPORT	18. SECURITY CLASSIFICATION OF THIS PAGE	19. SECURITY CLASSIFICATION OF ABSTRACT	20. LIMITATION OF ABSTRACT
UNCLASSIFIED	UNCLASSIFIED	UNCLASSIFIED	UNCLASSIFIED

HIGH ENERGY PULSED MICROWAVE SOURCES

FINAL REPORT

(Grant F49620-93-1-0103)

SUBMITTED TO:

Dr Robert Barker (202)-767-4904
Air Force Office of Scientific Research/NE
Building 410
Bolling Air Force Base
Washington, DC 20332-6448

SUBMITTED BY:

John A. Nation
Cornell University
Ithaca
N.Y. 14853

1-26-95

INTRODUCTION

The work summarized in this report covers research carried out at Cornell University during the period 2/01/93 to 10/31/94. During this period our research focussed on the generation of ultra high power microwave signals, especially on the elimination of sidebands from the amplifiers used, and in the latter period on the possibility of developing a tuneable high power amplifier. In this report we summarize both aspects of our program. Details of the results obtained may be found in the published papers, copies of which are appended to this report.

During the period of support a total of 5 papers were published and 7 conference presentations made on work arising totally or in part from this program. One student, Mr. Eric Kuang completed his Ph.D. degree. He is now employed by Motorola.

HIGH ENERGY PULSED MICROWAVE SOURCES

Sideband Control in TWT Amplifiers

This aspect of our program was initiated as a result of early successes in our research in obtaining ultra high power amplifier operation. Peak output powers in excess of 400 MW were obtained in X band at an electrical conversion efficiency of about 45%. One unexpected result was the discovery of asymmetrically located sidebands in the radiated power which were not due to trapped particles. Under the worst conditions 50% of the radiated power was in the sidebands and the remaining half at the input frequency. The sideband origin was traced to the existence of preferred frequencies in the amplifier operation. The preferred frequencies were associated with peaks in the transmission and reflection coefficients in short traveling wave tube amplifiers. The phenomenon has been described analytically and has been successfully simulation using the MAGIC code.

A number of techniques were thought of to suppress the unwanted sideband signals of which two were investigated experimentally. The first of these was the use of a transit time isolated amplifier and the second relied on establishing a well matched system in which reflections were unimportant. The second concept also relates to the use of a tuneable amplifier and will

be described later in this report.

The design of the transit time isolated amplifier was based on the use of an amplifier with a very low group velocity amplifying structure such that the time taken by a wave packet to propagate through the amplifier was comparable to that of the electron beam driver. The amplifier used was a two stage device with the first stage consisting of a dielectric loaded section with tapered ends to minimize unwanted reflections from the output and input of the amplifier. The first stage was followed by a sever in which the amplified electromagnetic power was absorbed while the space charge modulated beam wave was transmitted with only low loss. The EM wave was reconstructed in the ridged waveguide amplifier second stage amplifier section and amplifed at a rate in excess of 5 dB/cm. The very high growth rate goes with the low group velocity. The output of the amplifier was at the input frequency and there was no evidence of significant sideband development. Although we were extremely successful in this project we concluded that it was of only limited use due to two factors. The first of these relates to the difficulty of extending the technique to long ($> 1\mu sec.$) pulses and secondly due to the narrow bandwidth associated with low grouop velocity structures we have a very large interaction impedance and hence very high electric fields. Simulations showed that the wave electric fields at the rippled wall amplifier surfaces could be in excess of 250 MV/m. Although we found no evidence of breakdown in these experiments it is clear that the fields are sufficiently large that there is little hope of extending the t echnique to significantly longer microwave pulses.This work was published initially as a letter in Phys. Rev. Letters and more recently in detail in the special issue of the IEEE Plasma Sciences Journal. Copies of both of these papers are among the papers attached to this report.

One highlight of this work was the experimental measurement of the electron energy spectrum at the end of the amplifier. As predicted by theory accelerated as well as decelerated electrons were detected. The phenomenon of acceleration of electrons in a TWT amplifier is we believe new as it only significant in the case where very high electric fields are developed as a result of the wave interaction.

Tuneability of TWT Amplifiers

It would be very useful to be able to tune ultra high power traveling wave tube amplifiers over a frequency range of say $\pm$ 10% about the center frequency. In order to be able to achieve this one would probably wish to use an amplifier working in the opposite limit to the transit time isolated device indicated in the previous section. i.e. one would like to use a broad band device which has the additional advantages of lower growth rate, weaker electric fields and hopefully lower reflections from the ends of the amplifier sections. To accomplish this goal we designed a TWT amplifier with a passband of 1.5 GHz centered on 9 GHz. Extensive simulations were performed on the two stage amplifier structure to determine the gain characteristics when driven by a 1 MeV, 400-1000 A electron beam. The structure consisted of a 9 cell input structure with a 10 cell second stage, separated from the first by a silicon carbide sever, and used tapered input and output sections to reduce reflections. The simulations showed that with a fixed rf input of 30 kW gain was achieved over a 300 MHz bandwidth. With a 1000 A beam the gain peaked at 36.6 dB and a power of 140 MW, while with the lowe 400 A beam the gain dropped to 29.5 dB and the output power to about 28 MW. The bandwidth was $\sim$ 3% of the operating frequency and about $\sim$ 20% of the cold bandwidth of the structure.

Cold measurements indicated that the performance of the sever was not as good as that used in the simulations and that structure was shown in measurements of the reflection coefficient for the input section. Previous work has indicated that such reflections lead to the development of preferred operation frequencies which are manifested as sidebands in the amplifier output, or even with high currents to system oscillation at a preferred frequency. This led us to work on improving the sever characteristics. A reduction in the bore of the silicon carbide sever from 2 cm to 1.2 cm lead to improvements in the performance such that amplifier operation was possible at the lower current levels but not at the 1 kA level where the system oscillated. For the 400 A beam current, amplifier operation was demonstrated by changing the input power from 30 kW to 130 kW and observing a fourfold increase in the microwave output power from 6 to 24 MW, a value somewhat lower than indicated in the simulations but in the same range, and with an efficiency of only 6%. The measured gain was 23 dB compared

to the 29 dB predicted in the simulations. A check of the tuneability of the amplifier indicated that amplification was achieved over a frequency range extending from 9.1 to 9.4 GHz.

The work was terminated at this point due to funds running out and as a result of only achieving successful amplification at low beam currents. An effort, based mainly on programmatic needs in our DOE sponsored research, has been maintained since completion of this work to try to solve the problems arising from unwanted reflections. Since this is not directly related to tuneability but mainly to coupling signals in and out of the amplifier the results related to tuneability are limited. It does, however, show promise and is for the sake of completeness indicated here.

One of the main problems in eliminating sidebands is the reflections caused by the sever used to isolate the second stage of the amplifier from the first stage. This problem is common in circular cross section guides where the severs and waveguide terminations do not work as well as in rectangular guide. An alternate approach to the problem is to design an input section where the rf signal input at the start of the amplifier is completely extracted at the end of the section and a section of guide beyond cut-off is used to allow the space charge wave to propagate to the second stage where the microwavewave signal is reconstructed. This is similar to the approach used in klystrons where adjacent cavities are isolated from each other by guide operated beyond cut-off. The individual sections in this case are TWT's and do have gain so it is necessary to couple power out of the section to prevent oscillation.

Our first efforts were to design a rectangular sidearm output coupler guides to feed in and extract rf power from the input amplifier section. This was satisfactorily achieved by varying the length and iris diameter in the two end cavities. In the presence of the beam we discovered that the coupling was substantially reduced, far more in fact than one would expect from the dielectric loading due to the beam. The effect is probably due to capacitive lengthening of the amplifier section due to the presence of the beam. This resulted in oscillation of the input section at a frequency close to but not equal to that input. The effect could not be tuned away. As a result we have initiated work on a new input section in which we can achieve a relatively

broadband coupling, over a frequency range of about 200 MHz. This has been accomplished through the use of an amplifier section with the input and output sidearms separated from each other by only 2-3 cavities and with the rest of the amplifier extending beyond the coupling arms. This arrangement is not only relatively broadband but is tuneable under vacuum through the use of adjustable shorts in sections of guide opposite the input and output arms. In principle this coupling could be varied slowly over several seconds to match changes in the driving frequency of the amplifier. Transmission coefficients of over 0.95 have been achieved through the structure and 3 dB bandwidths approach 300 MHz. Beam loaded tests of the couplers and amplifiers are expected in the next few months.

Conclusions

The contract period extending from February 1993 through October 1994 has been productive. Techniques, such as the transit time isolated amplier have been successfully demonstrated as a means of suppressing sidebands in high power amplifiers. Work has also been initiated on new techniques to achieve this goal in long duration ($t \geq 1\mu sec.$)pulses in which the successive amplifer stages are isolated from each other by waveguides beyond cut-off. These devices have been cold tested but have not yet been tested under load. The work, albeit with the tuneability aspects de-emphaized, is continuing under DOE support.

During the One and a three-quarter year period covered by the contract a total of 5 papers have been published on this work in refereed journals and 5 and 2 papers respectively presented as conference papers and in oral presentations at meetings. The refereed journal papers are appended to this report.

PUBLICATIONS 1994

"Results from an X-band coaxial extended length cavity," T. J. Davis, L. Schächter, and J. A. Nation, *IEEE Trans. Plasma Sci.*, **22**, 504, (1994).

"Low group velocity traveling wave tube amplifier," E. Kuang, T. J. Davis, G. S. Kerslick, J. A. Nation and L. Schächter, *IEEE Trans. Plasma Sci.*,

22, 511, (1994).

"High power X-band microwave TWT amplifiers," E. Kuang, S. Naqvi, T. Davis, G. S. Kerslick, J. A. Nation, L. Schächter and Ge Zhang, Proceedings of the 10th International Conference on High Power Particle Beams, San Diego, CA, 20-24 June, 1994, pp 877-880.

PUBLICATIONS 1993

"High power microwaves at 9 GHz from an extended length cavity in a coaxial beam geometry," T. J. Davis, L. Schächter, and J. A. Nation, *Appl. Phys. Lett.* **63**, 1854 (1993).

"Analytical method for studying quasiperiodic disk loaded waveguide," L. Schächter, and J. A. Nation, *Appl. Phys. Lett.* **63**, 2441 (1993).

"Transit time isolation of a high power microwave amplifier," E. Kuang, T. J. Davis, G. S. Kerslick, J. A. Nation and L. Schächter, *Phys. Rev. Lett.* **71**, 2666 (1993).

"Development of high power X-band TWTS," E. Kuang, G. S. Kerslick, J. D. Ivers, L. Schächter and J. A. Nation, Presented at the 20th IEEE International Conference on Plasma Science, 7-9 June 1993, Vancouver, B.C., Canada.

"Repetitive electron beam source for high power microwave experiments," J. D. Ivers, G. S. Kerslick, R. Advani, L. Schächter and J. A. Nation, Presented at the 20th IEEE International Conference on Plasma Science, 7-9 June 1993, Vancouver, B.C., Canada.

"Two-stage, high power X-band amplifier experiment," E. Kuang, G. S. Kerslick, J. D. Ivers, J. A. Nation and L. Schächter, *Procedings of the 1993 IEEE Particle Accelerator Conference*, Washington DC, May 17-20, vol. 4, p.2687.

"Beam-wave interaction in quasi-periodic structures," L. Schächter and J. A. Nation, *Procedings of the 1993 IEEE Particle Accelerator Confer-*

ence, Washington DC, May 17-20, vol. 4, p.2684.

"*TM* FEL with a longitudinal wiggler and an annular beam," L. Schächter and J. A. Nation, *Procedings of the 1993 IEEE Particle Accelerator Conference*, Washington DC, May 17-20, vol. 4, p.2653.

"A compact, low cost modulator for rf sources," J. D. Ivers, G. S. Kerslick, J. A. Nation and L. Schächter, *Proceedings of the 1993 IEEE Particle Accelerator Conference*, Washington DC, May 17-20, vol. 2, p.1312.

Results From an X-Band Coaxial Extended Length Cavity

T. J. Davis, *Member, IEEE*, L. Schächter, and J. A. Nation, *Fellow, IEEE*

Abstract— **Experiments and simulations demonstrate high-power microwave generation at 9 GHz in a coaxial geometry. The 9 cm diameter annular electron beam is propagated between inner and outer drift tube conductors, a configuration which increases the beam current and reduces the structure fields from existing high-power sources. Since the TEM mode of the coaxial guide reduces the quality factor of small-gap cavities, especially at high frequency, the interaction is provided by an extended length cavity loaded with dielectric. A single 16 cm cavity generates 200 MW of power from the 400 keV, 7 kA electron beam. Although the cavity can oscillate at a number of resonances, a single mode is selected with 10–30 kW of input power from a magnetron. A coupler samples 25 MW of the power from the interaction region, precisely measured using a single-shot calorimeter. Simulations indicate that the efficiency of the device is limited to 7% by saturation effects, and can be improved by reducing the length of the cavity.**

I. Introduction

VIGOROUS effort in recent years has been applied toward the development of high peak power microwave amplifiers for particle accelerator and phased-array radar applications. Although relativistic klystrons [1], [2], gyroklystrons [3], traveling wave tubes [4] and free electron lasers [5] have extended the limits of radio frequency (rf) sources, no single device satisfies the stringent criteria of high frequency (>9 GHz) and high peak power ($\geq$ 100 MW) while maintaining amplitude and phase stability. The common approach in these devices is to propagate the electron beam in a single conductor waveguide, where the interaction occurs with the fundamental mode. As a consequence, the most serious limitation is the high fields imposed on the surface of the microwave structures, which often results in breakdown or pulse shortening [6] as the output power is increased. Reducing the surface fields below the threshold for field emission and breakdown is necessary to increase the peak power of any device, but is exceedingly dificult as the characteristic dimensions shrink for X and K frequency bands.

To alleviate the shortcomings of existing devices, we initiated a program to study microwave generation in a coaxial geometry. The cross section of our coaxial drift space is illustrated in Fig. 1; an annular electron beam is propagated within inner and outer drift tube conductors. By increasing the average diameter of the system, the surface fields are reduced because of the expanding volume in the microwave structures. A TM_{010} cavity in our coaxial arrangement, for instance, will reduce the maximum electric field by a factor of four over a standard pillbox TM_{010} resonator (for equivalent stored energy and gap length). In addition, the annular beam configuration allows the propagation of much higher beam currents; the beam cross sectional area increases with the average system diameter, and the limiting current is enhanced by the annular geometry. The limiting current for a thin annular beam in the coaxial drift tube may be calculated from

$$I_{\text{limit}} = 8.5\frac{(\gamma^{2/3}-1)^{3/2}}{\ln(r_b/r_i)}\left(1-\frac{\ln(r_b/r_i)}{\ln(r_b/r_o)}\right)\text{kA} \qquad (1.1)$$

where γ is the injection relativistic factor, r_b is the beam radius, and r_i, r_o are the inner and outer radii of the coax, respectively. For our 9 cm average system diameter, the limiting current is 48 kA, much higher than the 2-3 kA often found in pencil beam klystrons. In many respects, the coaxial beam is similar to a high aspect ratio sheet beam [7].

Of course, as the average system diameter is increased, waveguide modes will propagate in the drift space. Although the transverse magnetic (TM) modes can be cutoff in the coaxial guide by decreasing the separation distance between drift tube conductors, the fundamental transverse electromagnetic (TEM) mode and several transverse electric (TE) modes will propagate. Control of the transmission line TEM mode remains the most difficult task in the development of a coaxial microwave amplifier. The first high-power coaxial

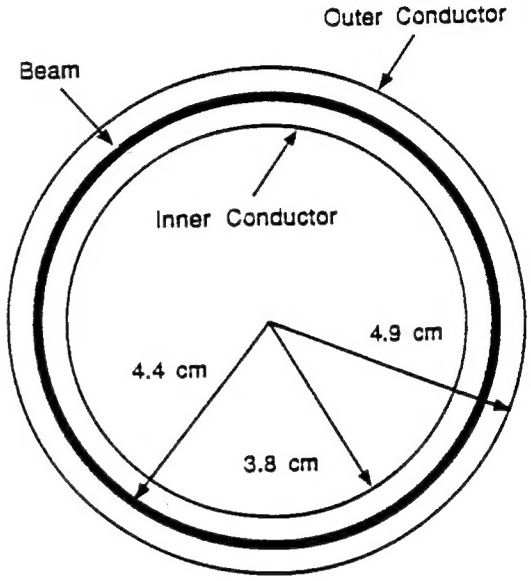

Fig. 1. Cross section of the coaxial drift space.

Manuscript received September 1, 1993; revised June 8, 1994.

The authors are with the Laboratory of Plasma Studies and School of Electrical Engineering, Cornell University, Ithaca, NY 14853 USA.

IEEE Log Number 9404584D.

source was demonstrated in 1970 [8], although research on coaxial traveling wave tubes had occurred as early as 1950 [9]. Recently, the coaxial geometry has been proposed to increase the peak power of an annular beam relativistic klystron [2], or as a simple extension of the dielectric Cerenkov interaction [10].

Section II will review the coaxial geometry in more detail. Since the TEM mode complicates the operation of a multi-cavity klystron, we study the possibility of an alternate extended cavity design in Section III. Experimental results from a single extended length cavity are presented in Section IV. Since the beam-cavity interaction is longitudinal, the device is easily studied using particle-in-cell (PIC) simulations; results from the MAGIC code are in excellent agreement with experiment, and are discussed in Section V. Finally, Section VI summarizes the results from the prototype cavity, and emphasizes possible improvements to the coaxial device.

II. Coaxial Description

The transmission line TEM mode is fundamental in the coaxial guide; the TM and TE modes are higher order. The cutoff frequencies of the TM modes can be determined by the boundary condition that $E_z = 0$ at the inner and outer conductors, or more formally

$$\frac{Y_n(k_c r_i)}{J_n(k_c r_i)} = \frac{Y_n(k_c r_o)}{J_n(k_c r_o)} \tag{2.1}$$

with $k_c = \omega_c/c$. To good approximation, this is equivalent to the condition that the separation of the conductors be an integer multiple of half wavelengths

$$f_c(\mathrm{TM}) \simeq \frac{mc}{2(r_o - r_i)}. \tag{2.2}$$

Therefore, in order to increase all TM mode cutoff frequencies above 10 GHz, the inner and outer conductors must be separated by 1.5 cm. Accordingly, most of the TE modes will be cutoff from a similar boundary condition on E_θ. For our coaxial system, an inner radius of 3.8 cm and an outer radius of 4.9 cm was selected. Naturally, however, the coaxial system will overmode as the average diameter increases. Several TE modes satisfy the condition that the circumference is an integer multiple of half wavelengths; their dominant B_z and E_r components are similar to a TEM wave traveling azimuthally around the guide.

Several cavity designs can be adapted to the coaxial geometry; two common resonators are a toroidal TM_{010} cavity with rectangular cross section, and a coaxial cavity made of sections of coaxial line [11]. To full advantage of the coaxial system, a cavity typically straddles the drift tube to provide the maximum electric field at the location of the beam. However, the effects of the TEM mode are readily apparent from the SUPERFISH plot of an example coaxial cavity in Fig. 2. With the beam aperture, the fields from the cavity extend into the drift tube, greatly modifying the cavity quality factor (Q) and effective gap length. This coupling to the TEM mode is markedly worse for high frequencies ($\sim$ 10 GHz); at L-band, it has been shown that a coaxial klystron design is still possible

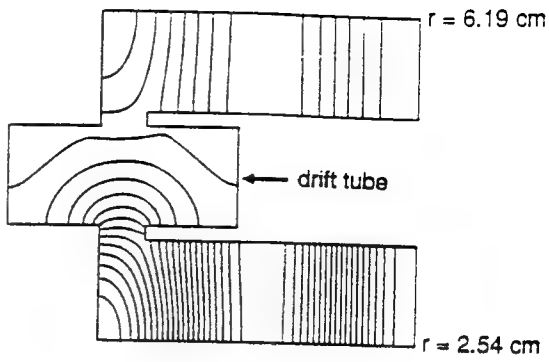

Fig. 2. SUPERFISH contours for a coaxial cavity opened to the drift tube. The cavity fields leak into the coaxial TEM mode, effectively reducing the cavity Q and increasing the gap length.

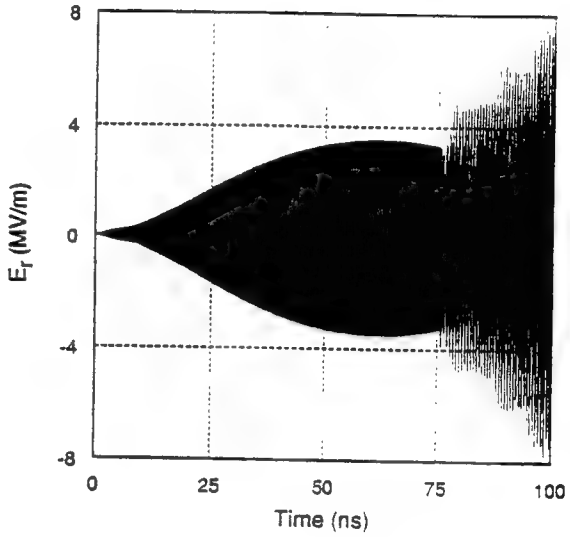

Fig. 3. Second cavity fields from a coaxial klystron simulation. Coupling from the first cavity through the TEM mode fills the second cavity prior to beam passage (75 ns). Little gain or enhancement of the input signal occurs, due to the coupling between cavities and the reduced cavity Q.

[12]. Often, the Q of a cavity is reduced from several thousand to several hundred from leakage to the TEM mode.

We have studied the effects of the TEM mode extensively in klystron simulations using the PIC code MAGIC. Fig. 3 is a plot of the simulation fields in the second cavity of a two cavity coaxial klystron. In the simulations, the beam is launched at 75 ns, after the input drive to the first cavity has settled to a dc level. Because of the TEM mode, energy leaks from the first cavity and prefills the second before the beam is launched. The initial cavity does create a small modulation upon the beam, which is not enhanced at the second gap. The resulting field levels in the second cavity are approximately the same as the first, also indicating little gain from the original signal. Two principle reasons for the loss of klystron efficiency are apparent; the Q of the cavities are degraded by radiative loss to the TEM mode, and the phasing of the two cavities is destroyed by electromagnetic coupling through the drift tube. We have examined a number of coaxial klystron configurations, in both experiment and simulation, none of which produce significant gain at 9 GHz. It may be possible to incorporate choke designs into the coaxial system to increase the Q of the resonators

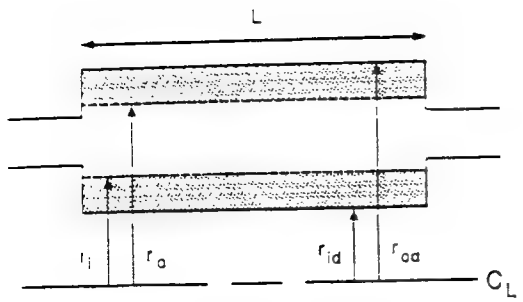

Fig. 4. Schematic of an extended length cavity loaded with dielectric. The cavity operates on the beam over many wavelengths through a slow wave interaction. Feedback occurs due to reflections from the cavity boundaries.

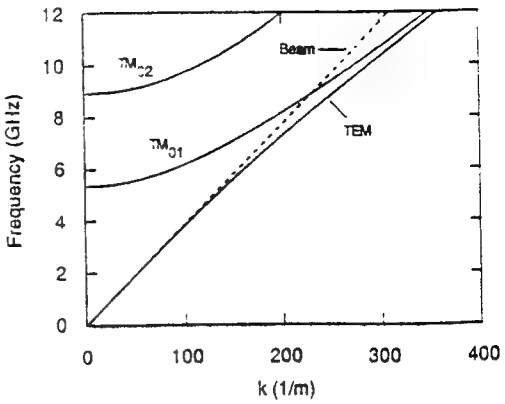

Fig. 5. Characteristic dispersion relation for a coaxial waveguide lined with dielectric.

[13], and the resulting efficiency of the small-gap cavity interaction. However, a high gain multi-cavity klystron is a difficult proposition for the coaxial geometry, especially at high frequency.

III. Extended Length Cavity

To reduce the effect of the TEM mode, however, we have selected a cavity design which relies on a high-gain slow wave interaction. A standard TM_{01} traveling wave tube (TWT) amplifier is difficult to implement in the coaxial geometry, because input coupling preferentially excites a TEM mode. More importantly, broadband excitation by the beam would likely result in sidebands or spurious output frequencies [4]. Fortunately, however, we can take advantage of reflections at the boundaries of the structure to reduce the sensitivity to input coupling and reduce the bandwidth of the interaction. Fig. 4 is a schematic of a short section of coaxial slow wave structure, with the loading provided by dielectric liners. Along the length of the structure, a strong convective interaction with the beam drives the TM_{01} mode. In the drift tube, the TM mode is cutoff; at the boundaries of the structure, therefore, some energy is transmitted to the TEM mode and some is reflected back into the interaction region. This feedback mechanism produces discrete frequencies of oscillation, effectively making the finite length slow wave structure an extended length cavity.

Finite length effects in TWT's have been studied previously [14], [15]. With feedback or reflections from the output, preferential gain peaks occur at the transmission peaks of the structure [14]. Since the gain is maximized at the transmission peaks, and minimized at the troughs, the effective bandwidth of the interaction is reduced. In simplified analysis, the gain-bandwidth product for a finite length structure is constant [15]. In experiments, reflections have been shown to reduce the bandwidth of a pencil beam TWT by several orders of magnitude [16]. Obviously, this concept is applicable to the coaxial geometry. Although the transmission analysis is slightly complicated by the TEM mode, the conclusions are qualitatively the same: a high-gain, narrow bandwidth interaction can be realized with an extended interaction length cavity. Consequently, the need for low Q (large bandwidth) small-gap cavities is eliminated.

We chose dielectric liners, rather than a metallic corrugation, for the prototype coaxial slow wave structure. Although normally avoided in high-power applications, dielectrics have been used successfully in several recent experiments [17], [18]. Because the breakdown strength depends strongly upon material properties, frequency, and pulse duration, the electric field at the dielectric surface should generally be limited to 10 MV/m in pulsed microwave devices [17]. However, the dielectrics greatly eased analysis and manufacture for the prototype device; the liners can be replaced in future experiments with a metallic periodic structure.

The dispersion relation for a dielectric-lined coaxial waveguide is found by applying the boundary condition $E_z = 0$ at the inner and outer conductors $(r_{\rm id}, r_{\rm od})$ and continuity of the tangential field components at the inner and outer radii of the dielectric liners r_i, r_o. The result for TM modes is derived as

$$\frac{k_1 T(r_i) Y_0'(k_2 r_i) - k_2 \epsilon T'(r_i) Y_0(k_2 r_i)}{k_2 \epsilon T'(r_i) J_0(k_2 r_i) - k_1 T(r_i) J_0'(k_2 r_i)} = \frac{k_1 S(r_o) Y_0'(k_2 r_o) - k_2 \epsilon S'(r_o) Y_0(k_2 r_o)}{k_2 \epsilon S'(r_o) J_0(k_2 r_o) - k_1 S(r_o) J_0'(k_2 r_o)} \quad (3.1)$$

where

$$T(r_i) = J_0(k_1 r_i) Y_0(k_1 r_{\rm id}) - J_0(k_1 r_{\rm id}) Y_0(k_1 r_i) \quad (3.2)$$

$$T'(r_i) = J_0'(k_1 r_i) Y_0(k_1 r_{\rm id}) - J_0(k_1 r_{\rm id}) Y_0'(k_1 r_i) \quad (3.3)$$

$$S(r_o) = J_0(k_1 r_o) Y_0(k_1 r_{\rm od}) - J_0(k_1 r_{\rm od}) Y_0(k_1 r_o) \quad (3.4)$$

$$S'(r_o) = J_0'(k_1 r_o) Y_0(k_1 r_{\rm od}) - J_0(k_1 r_{\rm od}) Y_0'(k_1 r_o) \quad (3.5)$$

with $k_1^2 = \omega^2 \epsilon / c^2 - k^2$ and $k_2^2 = \omega^2 / c^2 - k^2$ as the wavenumbers in the dielectric and vacuum, respectively.

The coaxial dispersion relation is similar to other dielectric waveguides, and is plotted in Fig. 5. The presence of the dielectric forces the TM_{01} mode to cross the beam line $\omega = kv$ at the synchronous frequency, where the strongest interaction occurs. In this case, a synchronous frequency of 9.0 GHz for a 400 keV, 7 kA beam is provided by a configuration with $\epsilon = 2.6$, $r_{\rm od} = 5.6$ cm $r_o = 4.9$ cm, $r_i = 3.8$ cm, and $r_{\rm id} = 3.2$ cm. In addition to the normal parabolic TM modes, the dispersion plot displays a TEM mode which is only slightly modified by the liners. For short wavelengths, all modes asymptote to $\omega = ck/\sqrt{\epsilon}$. As the dielectric constant of the liners increases, the slope of the asymptote decreases.

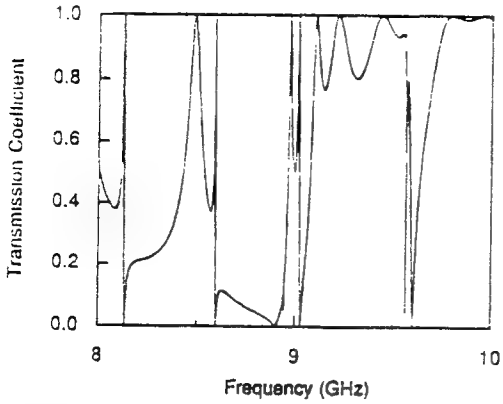

Fig. 6. Transmission through the extended cavity as a function of frequency for the 16 cm cavity. Only the transmission peaks arising from the TM_{01} mode are strongly driven by the beam.

Consequently, the synchronous frequency will decrease with increasing liner thickness or dielectric constant. A similar, but more complete, analysis of the lined coaxial waveguide is available elsewhere [10]. As in other geometries, the phase velocity $v_p < c$ condition forces the maximum field of the TM_{01} mode from the center of the guide to the liner surface.

It is possible to estimate the interaction frequencies of the extended cavity using the infinite structure dispersion calculation and the normal $kL = p\pi$ resonance condition (L is the length of the cavity, p is the integer number of half wavelengths). Since the infinite structure bandwidth is large, many frequencies satisfying this condition will effectively couple to the beam. The axial resonances can be predicted by matching the length L with appropriate k using a given p. The frequency is found from k using the dispersion relation. Using this procedure, we predicted that a cavity with $L = 16$ cm and $p = 12$ would oscillate at 9.06 GHz.

A self-consistent analysis of the extended cavity has also been performed [19]. The transmission peaks of the structure may be calculated assuming a TEM mode in the drift tube, and the TEM and TM modes in the cavity. Evanescent modes must be retained to properly match the boundary conditions. Fig. 6 is a plot of the transmission coefficient for the 16 cm extended cavity. The peak at 9.0 GHz confirms the first order design; additional peaks are also present due to the TEM mode. Since the beam couples predominantly to the TM modes, most of the spurious peaks are unimportant to the interaction. Incorporating macroparticles [20] within this framework of the cavity fields has demonstrated significant velocity modulation and bunching, especially when the synchronous frequency matches a transmission peak of the structure.

IV. Experiments

The experimental configuration is shown in Fig. 7. The 16 cm extended cavity, loaded with acrylic liners, was placed within the 3.8 cm inner and 4.9 cm outer radius coaxial drift tube. Magnetic field loops, which couple to beam and electromagnetic B_θ, were mounted on the drift tube wall and were used to diagnose the interaction. A portion of the power from the cavity was also sampled using a slot coupler. The 2.4 mm azimuthal slot was placed on the cavity

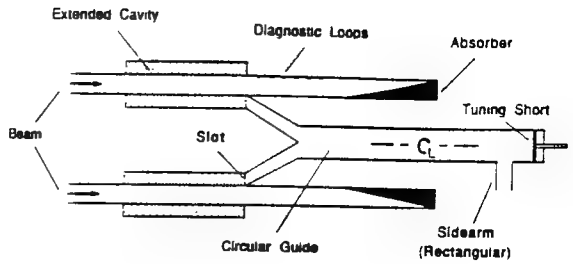

Fig. 7. Schematic of extended cavity experiment.

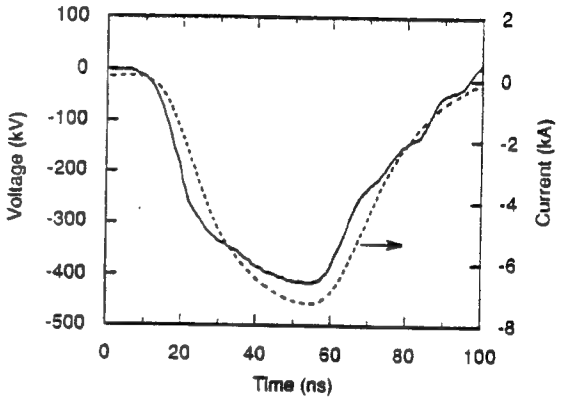

Fig. 8. Typical beam voltage and current waveforms. The nominal peak values for experiment were 400 keV, 7 kA.

downstream endplate, flush with the inner dielectric liner. The radiated power from the slot was coupled through a coaxial transition to 2.9 cm diameter circular waveguide. The circular guide was attached to normal X-band rectangular guide through a sidearm; a tuning short was adjusted to maximize the transmission at 9 GHz. The drift tube was terminated with a wedge-shaped silicon carbide absorber, cast from a pourable epoxy resin. Removing the absorber did not affect the characteristics of the output radiation.

A knife-edge field emission cathode was fully immersed in the uniform solenoidal field of 1 T, and produced a 2 mm thick electron beam. Shank emission was reduced by attaching the graphite cathode onto a conical mount. The voltage pulse to create the beam was generated by a modified Experimental Test Accelerator module [21]. Voltage and current waveforms from the beam, measured using a resistive voltage divider and set of Rogowski coils, respectively, are shown in Fig. 8. The typical peak beam parameters throughout the experiments were 400 keV and 7 kA, with an average beam diameter of approximately 9 cm.

Microwave emission typically occurred over 30–35 ns, centered about the period of peak beam power. Diagnostic traces from a magnetic field loop and the cavity coupler are shown in Fig. 9. The coupler pulse duration was often very brief ($\sim$ 10 ns), and always shorter than the signals from the drift tube probes; consequently, breakdown was suspected on the sidearm vacuum window. A dispersive line technique [22] was used to identify the frequencies of oscillation from the cavity. Digitized dispersive line traces from the cavity coupler are shown in Fig. 10. Without input power (a), the beam-cavity interaction produced distinct frequency components at

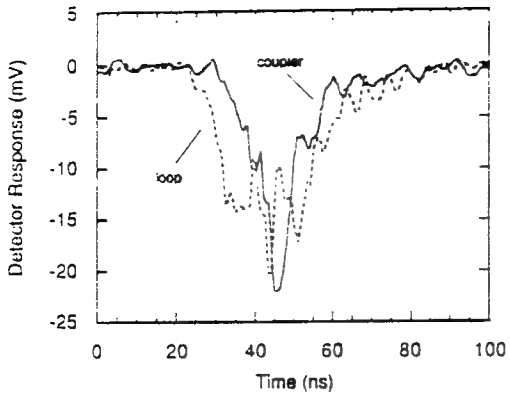

Fig. 9. Output waveforms from a diagnostic loop and the cavity coupler. Emission normally occurs for about 30 ns, centered around the period of peak beam power. The coupler traces are always shorter than the loop traces, indicating breakdown at the sidearm vacuum window.

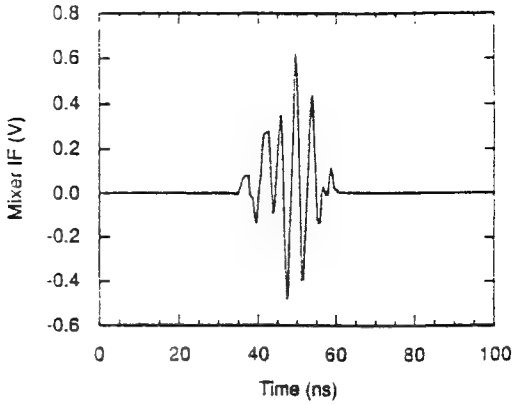

Fig. 11. Double balanced mixer output with external drive. The intermediate frequency from the mixer is monochromatic; the bandwidth of the radiation if found from the FFT to be approximately 100 MHz.

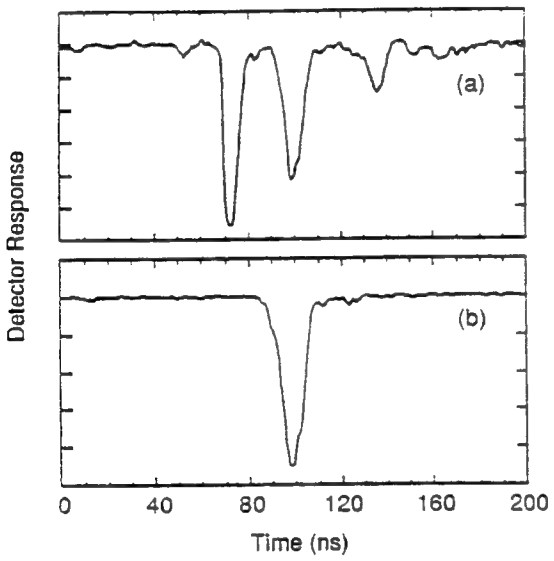

Fig. 10. Dispersive line traces from the cavity without (a) and with (b) input power from the magnetron. Without input power (a), resonances at 9.6,9.1, and 8.6 GHz are detected. A single mode is chosen at 9.1 GHz (b) with input powers in the range 10–30 kW.

9.6, 9.1, and 8.6 GHz. However, the cavity coupler was also used to input rf from an external magnetron, and thus select the interaction frequency. With input drive at 9.1 GHz, the cavity was locked to the center resonance (b). The precise input power level was difficult to measure due to reflections within the coupler, but was within the range 20–30 kW. Reducing the input power by a factor of two ($\sim$ 10 kW) made no difference in the output spectrum. In addition, the loop and coupler signal magnitudes did not vary with the magnitude of the external drive, and remained the same even in the absence of input. Therefore, the extended cavity operates as a single cavity oscillator.

A double balanced mixer provided additional confirmation of single mode operation. Fig. 11 displays the intermediate frequency (IF) resulting from a loop signal mixed with a local oscillator. With external drive, the downshifted signal was monochromatic. The fast Fourier transform (FFT) of the mixer IF revealed a bandwidth of approximately 100 MHz, indicating that the active feedback mechanism significantly narrowed the interaction bandwidth.

Since the sidearm attached directly to rectangular waveguide, the coupled power could be monitored with calibrated detectors. The power measured using this method could not be trusted, however, since breakdown was suspected on the sidearm window. To provide an independent measure of the coupled power, therefore, a hot-air calorimeter was inserted in place of the sidearm. The calorimeter is based on previous designs [23]; absorbed microwave energy is converted to a pressure rise within the calorimeter chamber. Our implementation increased the sensitivity to 1.25 J/V by reducing the chamber size, and limited the VSWR below 1.2 over the range 8.75–9.25 GHz. Because of the mechanical design of the coupler, no input power to the cavity was available with the calorimeter in place; nevertheless, the cavity oscillates to the same power level. The coupled power was measured up to a maximum of 25 MW, within 10–20%, using the calorimeter. A monitor loop within the coupler showed no evidence of breakdown in the absence of the sidearm window.

V. Simulations

As a final confirmation, the experimental results were compared with an extensive set of MAGIC simulations. The extended cavity is easily modeled with 6 mm liner regions of $\epsilon = 2.6$ as in the original design. The cavity is placed within sections of coaxial drift tube, where absorbing boundaries are used to accurately measure the output radiation. A 2.4 mm aperture connects the inner half of the cavity to a section of coaxial line, and serves as a good approximation to the slot coupler. The simulations used a cold beam with no thermal spread or variation in time.

The phase space of the macroparticles from simulation is shown in Fig. 12. Strong bunching is apparent from the velocity modulation along the length of the cavity. The phase space does, however, demonstrate that the interaction saturates, since particles are re-accelerated by the radiation field toward the end of the cavity. Accordingly, the efficiency of the device is reduced as microwave energy is drained to re-energize the particles. During the simulation, the maximum electric field of 28 MV/m occurs at the outer dielectric surface. This field

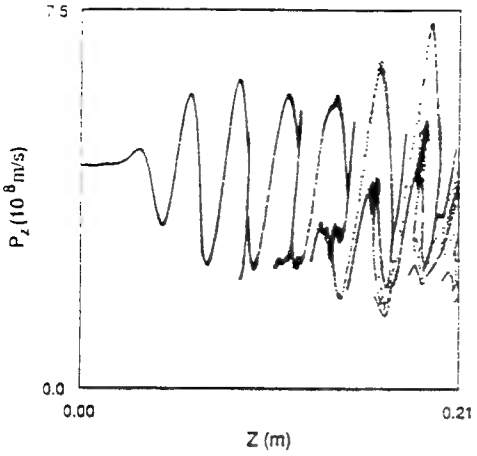

Fig. 12. The phase space of the cavity interaction from MAGIC simulations, plotted as the normalized axial momentum $P_z = \gamma v$. A significant amount of velocity modulation is created by the interaction. However, saturation results in particle re-acceleration, limiting the efficiency of the device.

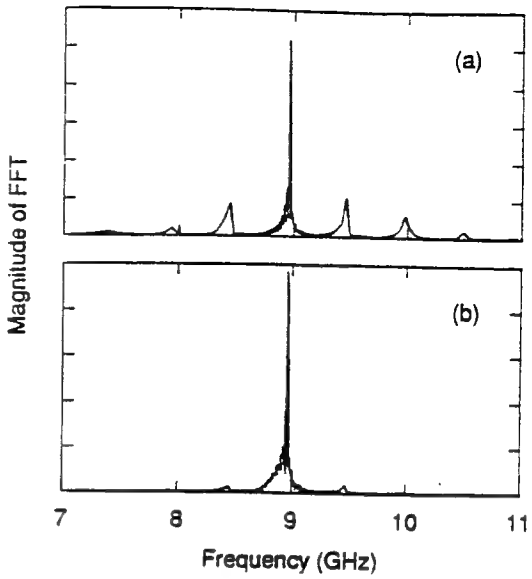

Fig. 13. FFT's of the coupler fields from simulations without (a) and with (b) 25 kW of input drive power. The interaction is again locked to a single resonance (b), with coupled output power of 27 MW.

exceeds the threshold for most materials, and is corroborated by experimental evidence of damage on the liner.

Simulations were run for 100 ns to reduce the frequency resolution within 10 MHz. FFT's of the radial electric field across the coupler coaxial line are shown in Fig. 13. Without input drive, the six discrete frequencies in (a) is evidence of the coupling over many axial resonances in the cavity. However, the boundary condition for the coaxial line of the coupler functions to launch power into the cavity, while absorbing any output from the interaction. As seen in (b), the spectral quality of the output radiation improves substantially using 25 kW of input power at the 8.96 GHz resonance. One mode, at the drive frequency, now dominates the interaction. For input powers in the range 10–100 kW, the output power in the spurious cavity resonances remains negligible. The magnitude of the coupled power in the dominant mode is also independent of the input drive levels, confirming that the device operates as a cavity oscillator.

By diagnosing the coaxial voltage, the simulations provide an accurate measure of the TEM mode output power. From simulation data, for 25 kW of input drive, the rf power through the coupler is measured to be 27 MW. This result is in excellent agreement with the 25 MW obtained from calorimeter experiments. Although the coupled output power can be measured with accuracy, this is not the total microwave power created by the interaction. As predicted, a significant fraction is lost to the TEM mode in the drift tube. The total rf power can be approximated by the loss in kinetic energy of the beam as it traverses the entire interaction region. From particle diagnostics before and after the cavity, the beam power in simulation decreases by 200 MW. Without a dielectric structure, no such decrease occurs; therefore, this power loss represents the total beam power converted to microwaves. Accordingly, the beam—rf conversion efficiency for the extended cavity is 7%.

VI. Conclusion

To summarize, we have demonstrated high-power microwave generation in the coaxial geometry using an extended length cavity. The 16 cm cavity, loaded with dielectric liners to slow the wave phase velocity, generates 200 MW of microwave power at 9 GHz from a 400 keV, 7 kA electron beam. The cavity is locked to a single resonance using 10–30 kW of input power from a magnetron. The reduced 100 MHz bandwidth of the interaction is a result of reflections from the boundaries of the finite length structure. A coupling system sampled 25 MW of power from the cavity, precisely measured using a calorimeter. The coupled power represents only a portion of the total created by the interaction. The overall 7% efficiency of the device is limited by saturation effects.

Obviously, the output of the device could be improved by alleviating saturation. After saturation was observed in the 16 cm cavity, a 12 cm design was investigated in simulation. From the $kL = p\pi$ condition, 12 and 16 cm cavities oscillate at the same frequency with different axial mode numbers. Fig. 14 displays the phase space from simulation of the 12 cm cavity, which operates at 8.93 GHz. Since particle re-acceleration, and thus saturation, is reduced, both the coupled and total output power are significantly improved from the 16 cm cavity. From simulation diagnostics, 200 MW can be extracted from the coupler and 450 MW is created in the interaction region. Accordingly, the efficiency of the device increases to 16%. The output spectrum from the shortened cavity is also improved from the original design. Although the high-field levels from the 12 cm cavity would further stress the dielectric liners, shorter cavity designs should be incorporated to improve the output power. Again, only a portion of the total power is coupled through the slot; future efforts must focus on the efficient extraction of the microwave energy.

Although the extended cavity operates as a single cavity oscillator, it may be possible to incorporate several cavities in a more conventional amplifier configuration. Provided that an initial modulation is created upon the beam, using a short extended cavity or even a small-gap klystron cavity, the 12 cm cavity can function as the output structure. A demonstration

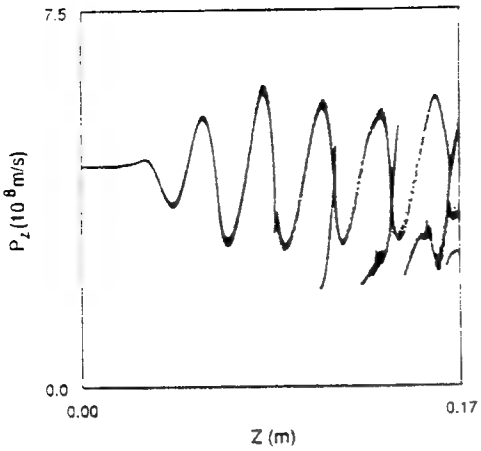

Fig. 14. Phase space from the 12 cm cavity simulation. Saturation is greatly reduced, leading to improved output power and efficiency.

simulation with 8 cm input and 12 cm output cavities has been performed. Although the output power remains identical to the single 12 cm cavity, the output spectrum is significantly improved by detuning of the spurious cavity resonances. Further study of this configuration is warranted to determine the required level of input drive and the optimal separation of the cavities.

ACKNOWLEDGMENT

The MAGIC code was supplied by Mission Research Corporation through an agreement with AFOSR.

REFERENCES

[1] M. A. Allen, *et al.*, "High-gradient electron accelerator powered by a relativistic klystron," *Phys. Rev. Lett.*, vol. 63, no. 22, pp. 2472–2475, 1989.

[2] Y. Y. Lau, M. Friedman, J. Krall, and V. Serlin, "Relativistic klystron amplifiers driven by modulated intense relativistic electron beams," *IEEE Trans. Plasma Sci.*, vol. 18, no. 3, pp. 553–569, 1990.

[3] W. Lawson, J. P. Calame, B. P. Hogan, M. Skopec, C. D. Striffler, and V. L. Granatstein, "Performance characteristics of a high-power X-band two-cavity gyroklystron," *IEEE Trans. Plasma Sci.*, vol. 20, no. 3, pp. 216–223, 1992.

[4] D. Shiffler, J. D. Ivers, G. S. Kerslick, J. A. Nation, and L. Schächter, "Sideband development in a high-power traveling-wave tube microwave amplifier," *Appl. Phys. Lett.*, vol. 58, no. 9, pp. 899–901, 1991.

[5] M. E. Conde and G. Bekefi, "Experimental study of a 33.3-GHz free-electron-laser amplifier with a reversed axial guide magnetic field," *Phys. Rev. Lett.*, vol. 67, no. 22, pp. 3082–3085, 1991.

[6] M. A. Allen, *et al.*, "Relativistic klystron research for high-gradient accelerators," in *EPAC: 1988 European Particle Accelerator Conf.*, Rome, Italy, 1988, pp. 121–126.

[7] G. Providakes, J. A. Nation, and M. E. Read, "Microwave generation using sheet relativistic electron beams," *IEEE Trans. Microwave Theory Tech.*, vol. 25, no. 6, pp. 563–566, 1977.

[8] J. A. Nation, "On the coupling of a high-current relativistic electron beam to a slow wave structure," *Appl. Phys. Lett.*, vol. 17, no. 11, pp. 491–494, 1970.

[9] G. C. Dewey, P. Parzen, and T. J. Marchese, "Periodic-waveguide traveling-wave amplifier for medium powers," in *Proc. IRE*, vol. 39, no. 2, pp. 153–159, 1951.

[10] E. P. Garate, A. Fisher, and W. T. Main, "Coaxial configuration of the dielectric cerenkov maser," *IEEE Trans. Plasma Sci.*, vol. 18, no. 5, pp. 831–836, 1990.

[11] S. Ramo, J. R. Whinnery, and T. Van Duzer, *Fields and Waves in Communication Electronics*, New York: John Wiley & Sons, 1984, ch. 10.

[12] J. Krall, M. Friedman, Y. Y. Lau, and V. Serlin, "Relativistic klystron amplifier IV: simulation studies of a coaxial-geometry RKA," in *Proc. SPIE Intense Microwave and Particle Beams II*, Los Angeles, CA, vol. 1407, 1991, pp. 23–31.

[13] D. U. L. Yu and P. B. Wilson, "Sheet-beam klystron rf cavities," to be published in the *Proc.of the 1993 Particle Accelerator Conference*, Washington, D.C., 1993.

[14] S. A. Cohen, "Traveling-wave tube gain fluctuations with frequency," *IRE Trans. Electron Dev.*, vol. 4, no. 1, pp. 70–78, 1957.

[15] L. Schächter, J. A. Nation, and G. Kerslick, "On the bandwidth of a short traveling wave tube," *J. Appl. Phys.*, vol. 68, no. 11, pp. 5874–5882, 1990.

[16] D. Shiffler, J. A. Nation, and G. S. Kerslick, "A high-power traveling wave tube amplifier," *IEEE Trans. Plasma Sci.*, vol. 18, no. 3, pp. 546–552, 1990.

[17] W. T. Main, E. Garate, J. Weatherall, and R. Cherry, "A frequency-locked, high-power, X-band dielectric Cerenkov maser," *IEEE Trans. Plasma Sci.*, vol. 20, no. 3, pp. 281–287, 1992.

[18] W. Main, R. Cherry, and E. Garate, "200 MW S-band dielectric Cherenkov maser oscillator," *Appl. Phys. Lett.*, vol. 55, no. 15, pp. 1498–1500, 1989.

[19] L. Schächter, T. J. Davis, and J. A. Nation, "A proposed extended cavity for coaxial relativistic klystrons," to be published in the *Proc.of the 9th Inter. Conf.on High-Power Particle Beams*, Washington, D.C., 1992.

[20] L. Schächter and J. A. Nation, "Cerenkov traveling-wave tube with a spatially varying dielectric coefficient," *Phys. Rev. A.*, vol. 43, no. 7, pp. 3785–3794, 1991.

[21] R. E. Hester, *et al.*, "The experimental test accelerator (ETA)," *IEEE Trans. Nucl. Sci.*, vol. 26, no. 3, pp. 4180–4181, 1979.

[22] J. A. Nation, "A simple technique for single shot microwave spectrum analysis," *Rev. Sci. Instrum.*, vol. 41, no. 7, pp. 1097–1098, 1970.

[23] C. B. Wharton, L. M. Earley, and W. P. Ballard, "Calorimetric measurements of single-pulse high-power microwaves in oversized waveguides," *Rev. Sci. Instrum.*, vol. 57, no. 5, pp. 855–585, 1986.

Timothy J. Davis received the B.S. degree in engineering science and mechanics from the Pennsylvania State University in 1986. During his undergraduate studies, he worked on fluid experiments and measurement techniques as an undergraduate assistant at the Applied Research Laboratory. He proceeded to Cornell University where he obtained his Ph.D. in electrical engineering in August 1993, with emphasis in electromagnetics and plasma physics.

He is currently employed by a start-up venture in Ithaca, NY.

Dr. Davis is a member of the IEEE, the American Physical Society, the American Vacuum Society, and Tau Beta Pi.

Levi Schächter graduated from the Technion in electrical engineering: B.Sc.-1983, M.Sc.-1985 and D.Sc.-1988 in addition to a B.A. in physics in 1985. He was with the Department of Electrical Engineering between 1988–1989 after which he started a four year visit to Cornell University.

At present Dr. Schächter is a Senior Lecturer with the EE Department at Ben-Gurion University. His areas of research interest are radiation sources based on electron beams, electron beam generation and novel schemes for particle acceleration.

John A. Nation (M'68–SM'76–F'89) received the B.Sc. and Ph.D. degrees in physics from Imperial College, University of London, in 1957 and 1960 respectively.

From 1960–1962 he worked at the Comitato Nazionale per L'Energia Nucleare Laboratoy in Frascati, Italy. He returned to the U.K. in 1962, working at the Central Electricity Generating Board Research Laboratories until 1965 when he joined the faculty of the School of Electrical Engineering at Cornell University, Ithaca, NY, where he is presently Professor of Electrical Engineering and a member of the Laboratory of Plasma Studies. He served as Director of the School from 1984–1989. His current research interests are in the applications of pulse power technology to high-power microwave generation and particle accelerators.

Prof. Nation is a holder of the IEEE Centennial Medal and a Fellow of the American Physical Society.

Low Group Velocity Traveling Wave Tube Amplifiers

E. Kuang, T. J. Davis, J. D. Ivers, G. Kerslick, J. A. Nation, and L. Schächter

Abstract—**We report experimental and theoretical results from research into high power X-band traveling wave tube amplifiers designed to eliminate sidebands caused by reflections from the output of such structures. These amplifiers have a low energy velocity, such that the time it takes a wave to be reflected from the output to the input is of the order of, or greater than, the electron beam pulse duration. The elimination of sidebands and the effects of reflections is achieved by this transit time isolation. The bandwidth of the output spectrum is limited by the low pass-band of the periodic structures. Such amplifiers have been operated at power levels of up to 160 MW at 9 GHz for 50 ns pulse durations.**

I. Introduction

RESEARCH has been carried out over the last few years into a variety of high power microwave sources. One of the driving forces for this work is the proposed next linear collider, an electron-positron collider which will require the development of microwave sources capable of generating $\sim$ 200 MW/m of acceleration structure. At these power levels acceleration gradients of 100 MV/m are expected for X-band operation with pulse durations in excess of 100 ns. An electron-positron collider, or any phased array, requiring high power microwave sources will need to be phase stable and operate efficiently with single frequency output. The general trend in this area of research [1] is to expand beyond the S-band klystron to frequencies in the range 10–30 GHz. The main reason for this trend is that the microwave power necessary to produce a given accelerating gradient varies approximately as the inverse of the operating frequency squared ($P \propto f^{-2}$). Thus an increase by a factor of 3 in the frequency can lower the necessary power by one order of magnitude. However, an increase in the frequency is accompanied by a corresponding reduction in the physical dimensions of the klystron's cavities and drifting region. This becomes a significant drawback when rf breakdown is considered. The smaller the volume of the cavity, for a given stored energy, the larger the electric fields and thus the probability of rf breakdown increases. This problem becomes acute in the extraction cavity.

In order to overcome this problem, and reduce the local field gradients, it is possible to replace the extraction cavity, or in principle, the entire klystron, by a traveling wave structure—e.g. a disk loaded waveguide. Unlike the klystron where the cavities are electromagnetically isolated (by the drift region which is below cutoff) the traveling wave structure is a set of coupled cavities, which are separated from each other by short sections of guide which may be above or below cutoff. In this case the beam-wave interaction is distributed along the entire interaction length whereas in a klystron it is limited to the close vicinity of the cavity. The advantage of traveling wave extraction sections is that they can be designed to have bandwidths comparable to the main amplifier but with a larger internal radius and the electric field on the walls can thus be reduced for a given output power.

In this paper we describe the design and performance of a high output power narrow band TWT. In previous work, carried out in our laboratory, we have succeeded in generating very high power microwave sources ($\sim$ 400 MW at $\sim$ 9 GHz) but reflections from the output section have lead to the development of sidebands which can carry up to $\sim$ 50% of the radiated power. In this paper we describe results obtained on a low group velocity TWT amplifier. The design concept is based on the transit time isolation of the input from the output of the device [2]. In this regime, even if reflections are present their effect on the generation of sidebands will be unimportant as the feedback time exceeds the beam pulse duration.

In the following sections we review theoretical and experimental data previously obtained using wide band amplifiers. This is followed by an account of the performance of the new narrow band device. The paper concludes with a discussion of limitations set by the high interaction impedance of the amplifier.

II. Review of Previous Experimental Results

The use of traveling wave amplifiers for the production of high power microwave radiation in X-band has been reported previously [3]-[6]. In a single stage amplifier, consisting of a section of sinusoidally corrugated waveguide, driven by a 0.85 MV, 0.8–1.6 kA, 100 ns pulse duration electron beam, total power levels of up to 120 MW, with gains of 33 dB and with bandwidths of $\sim$ 30 MHz, were measured. Measurements show that the amplified signal is phase stable to within the $\pm$ 8° limit set by the discriminator diagnostic [5]. Beyond these power levels the system was noisy and prone to oscillation. In addition, for output powers above 80 MW the output spectrum showed the development of asymmetric sidebands.

To avoid oscillation, a two stage severed amplifier was developed. This device consists of two rippled wall waveguides isolated from each other by a sever, consisting of a lossy section of waveguide operated below cutoff. The space charge waves, which develop along the beam in the first stage, propagate through the sever whereas the electromagnetic mode

Manuscript received September 1, 1993; revised June 9, 1994. This work was supported by the Department of Energy and the Air Force Office of Scientific Research.

The authors are with the Laboratory of Plasma Studies and School of Electrical Engineering, Cornell University, Ithaca, NY 14853 USA.

IEEE Log Number 9404585D.

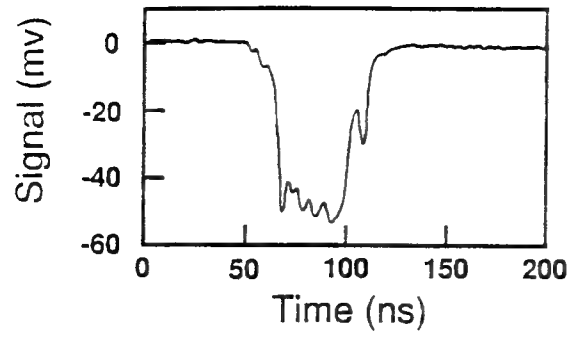

(a)

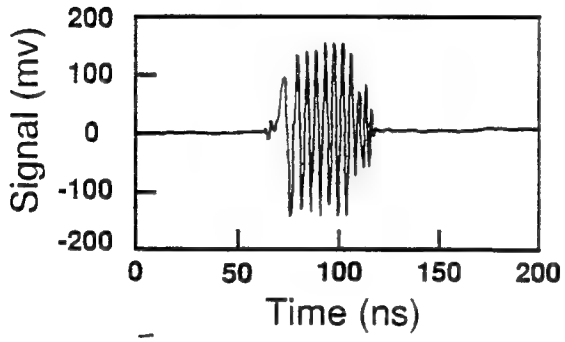

(b)

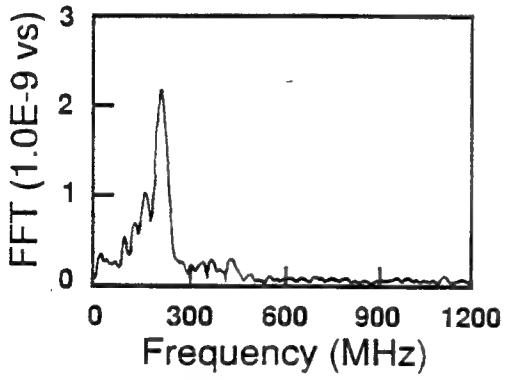

(c)

Fig. 2. Single stage dielectric amplifier outputs. (a) Detected output signal, (b) heterodyned signal, (c) FFT of heterodyned signal.

observed, however the signal is noisy, exhibits multiple output frequencies and at the highest power levels ~ 150 MW is subject to some pulse shortening. In our two-stage amplifier experiments, the length of the first stage is restored to 30 cm to eliminate possible rf breakdown problems. Fig. 2 shows an output power waveform, together with the heterodyned signal and the FFT. Note that the output power envelope is relatively flat and is sustained for the length of the electron beam pulse, indicating that no rf breakdown is occurring. The FFT shows a single frequency output. The output power as a function of input frequency is shown in Fig. 3 illustrating the broad gain-bandwidth curve for the dielectric single stage amplifier, characteristic of operation at low power with only modest gains. The gain measurements quoted are ±1 dB.

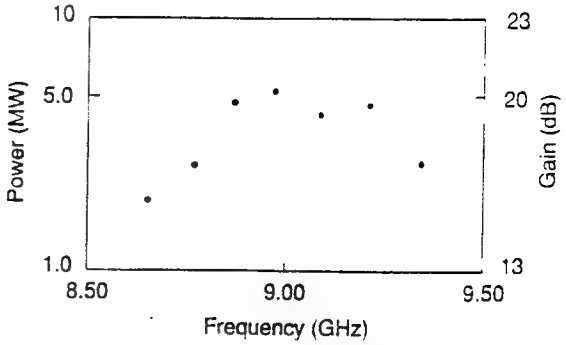

Fig. 3. Measured frequency response of the single stage amplifier, showing broad bandwidth characteristic. Gain measurements ±1 dB.

B. Two-Stage Amplifier Performance

Measured output signals for the two stage amplifier are shown in Fig. 4. Note that, as in the single stage device, the output pulse is of the same duration as the electron beam. The pulse shape is, however, somewhat degraded. The single frequency feature of the FFT shows that the sidebands, seen in wider bandwidth structures at these power levels, have been eliminated. The output power as a function of input magnetron frequency (input power ~ 50 kW) is presented in Fig. 5, which shows a 3 dB bandwidth of about 40 MHz for this device. Output powers of 160 MW at 8.87 GHz have been measured for the complete beam pulse duration (~ 50 ns). The frequency of the output signal was found to be independent of the axial magnetic guide field strength. Slightly higher powers ~ 180 MW (Fig. 5) have been obtained with shorter, 30 ns pulse durations.

Results from the calorimeter, also shown in Fig. 5, correlate well with that of far field measurement up to 65 MW. Above this power level the calorimeter pressure transducer saturates, and modifications will be required to extend the range.

Following theoretical work carried out into coupling structures [14] we found that the measured power output from the two stage amplifier depends strongly on the design of the last section of the narrow band structure. With a uniform iris thickness of 0.6 cm for all ten periods the maximum output power measured in the far field is 60 MW. When the thickness of the last iris is reduced to 0.1 cm the output reaches the 160 MW level quoted above. Qualitatively this may be attributed to attenuation in the 6 mm output iris section, which is below cut-off at the wave frequency.

Momentum measurements confirm the PIC and 1-D code results that the electron energy is strongly modulated. The time integrated electron energy spectrum is shown in Fig. 6 for three sets of conditions. Fig. 6(a) shows the spectrum of the injected electron beam. In Fig. 6(b) we show the spectrum without any rf input. In this case the wave grows in the amplifier structures from noise, causing a substantial change in the electron momentum distribution. The main peak is at the injection energy of 900 kV, but there is also a significant component at 250 kV. This component is not present in the absence of the amplifier structures and is clear evidence that the wave growing from noise has extracted energy from the electron beam. The spectrum with rf input, Fig. 6(c), shows

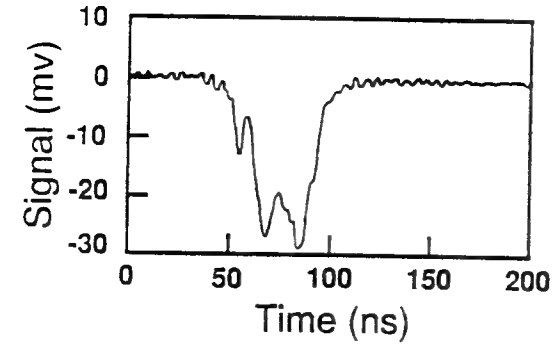

(a)

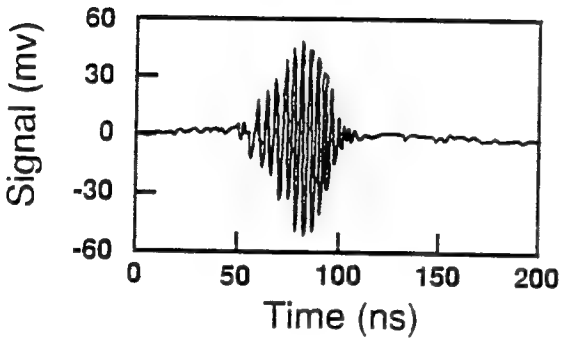

(b)

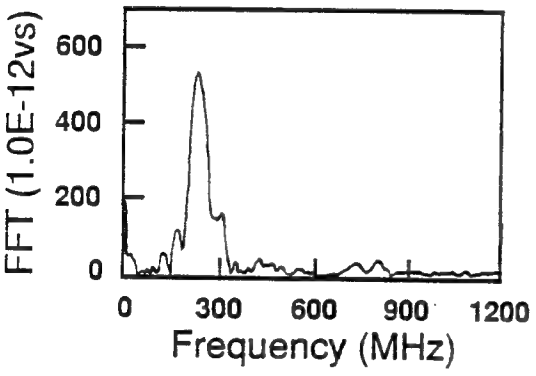

(c)

Fig. 4. Two stage narrow band amplifier outputs. (a) Detected output signal, (b) heterodyned signal, (c) FFT of heterodyned signal.

a larger spread in electron energies extending from 0.25–2 MV with a clear component at higher energy than that of the injected beam. The wide spread of the electron energy agrees well with the simulation results.

VI. Discussion and Conclusion

Although we have accomplished our main goal, namely the elimination of sidebands from the spectrum of a high power traveling wave amplifier, there is one problem which remains to be addressed. Both the analytic simulations and MAGIC code results predict a very high gain per cell in the narrow band structure, significantly higher than the 160 MW observed. We attribute this discrepancy to the effect of the

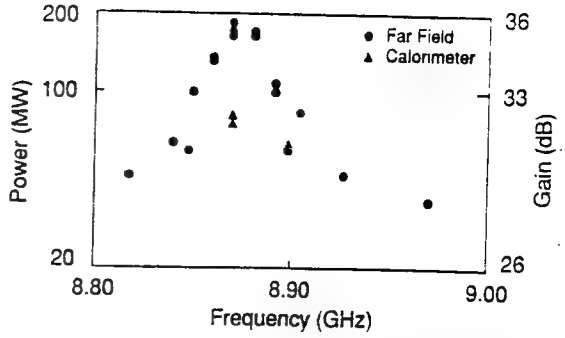

Fig. 5. Measured frequency response of the two stage amplifier. The triangles indicate calorimetric data and the circles data obtained from the far field measurements. The calorimeter output saturates at about 65 MW. Gain measurements ±1 dB.

sever, which attenuates (-25 dB) the electromagnetic mode but its effect on the space-charge modes is not known. In order to examine this qualitatively we have used the 1-D code outlined earlier. For modeling we have used a 30 cm long dielectric amplifier operated at 8.88 GHz and driven by a 1 kA, 1 MV, 0.3 cm radius pencil beam. The interaction impedance for this structure is calculated and found to be 0.4 kΩ. Using these parameters we compute the gain of this first stage to be approximately 27 dB.

We know that it is the slow space charge wave which is actually amplified in the interaction process. The sever attenuates only the electromagnetic wave and so we assume it has no significant effect on the *amplitude* of the space charge wave. However the wave phase, relative to the beam bunching, depends critically on the sever length. We therefore use the code to examine the effect on the gain of changes in the wave phase in transit through the sever.

Before we present the results of the simulation we note that for space charge wave propagation along a strong axial magnetic field the current density is related to the longitudinal electric field by

$$J_z = -j\omega\epsilon_0 \frac{\omega_p^2}{(\omega - kV)^2} E_z \tag{6}$$

where ω_p is the relativistic plasma frequency. In an uniform pipe k is real therefore J_z and the longitudinal electric field E_z are orthogonal ($-90°$) in phase whereas in a traveling wave structure the slow space-charge wave has a complex wavenumber $k = \omega/V + \frac{1}{2}K_0(1+j\sqrt{3})$ and the angle between E_z and J_z is $-60°$. It is the phase between the current density and the electric field which controls the actual energy transfer in the system (recall the $J_z E_z$ term in Poynting theorem).

In the simulation the NBS was assumed to be 12 cm long with a calculated interaction impedance of 5 kΩ ($R_{\text{in}} = 0.62$ cm). The particle distribution on both sides of the transition point (the sever is modeled with zero width) was assumed to be identical as was the wave amplitude. However, the phase of the field is shifted. Fig. 7 illustrates how the gain develops along the entire system for four cases. Note that the gain of the second stage is drastically altered by this phase shift. This effect is even more clearly revealed in Fig. 8 where we present the gain and the power as a function of the phase shift. For

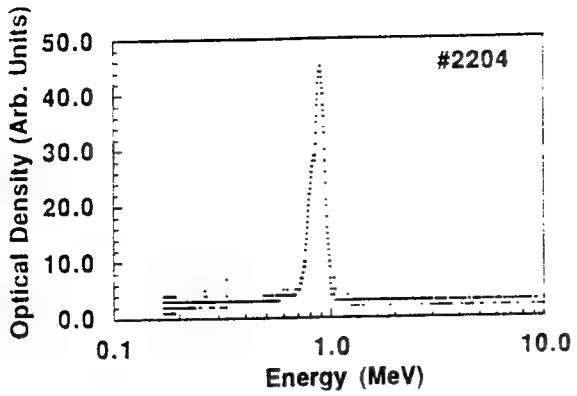

(a)

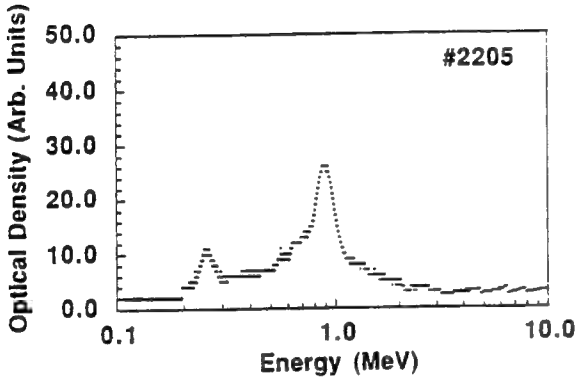

(b)

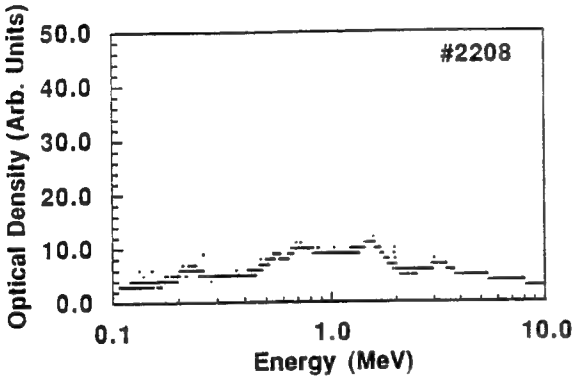

(c)

Fig. 6. Electron energy spectra at the amplifier output. (a) Injected electron spectrum, (b) output energy spectrum without rf input, (c) output energy spectrum with rf input.

an input power of 25 kW the power can vary from 190 MW to a few MW's as the phase was shifted from 300° to 150°.

We conclude that the sever can affect the relative phase between the current density and the longitudinal E-field. Its effect should be carefully considered, not only for electromagnetic isolation of the input from the output, but also to optimize its influence on the space charge mode(s).

In summary we have successfully developed a transit time isolated traveling wave tube amplifier capable of delivering an output power of 160 MW in a 50 ns pulse. Whether this level

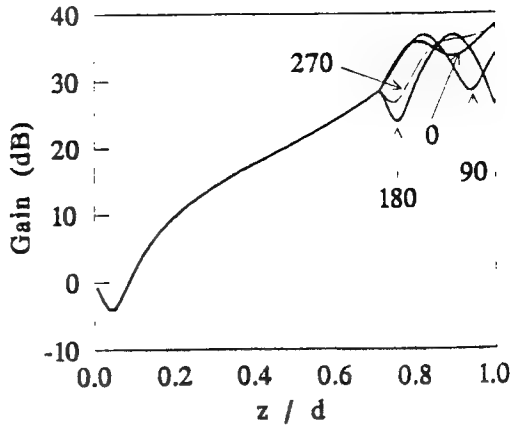

Fig. 7. Gain versus distance in a two stage amplifier with four different phase shifts occurring between the stages at $z/d = 0.7$.

of performance can be extended to longer duration pulses is not clear at this time. It is clear, however, that this technique is not likely to work with pulse durations in excess of one microsecond.

In the work presented we used a dielectric loaded guide for the first stage of the TWT. The choice of this amplifier configuration was made purely for the convenience of its large bandwidth. A rippled wall amplifier could and should be used to replace the dielectric first stage. A major limitation in the use of the narrow bandwidth second stage amplifier is the fact that the gradients on the surface of the metallic structure are very high (larger than 200 MV/m at the output). This is a direct result of the high interaction impedance and removes some of the breakdown advantages over the klystron. In principle there are steps which may be taken to alleviate this limitation. These include the use of narrow band structures with comparable bandwidths, but with a larger internal radius. This may be accomplished by keeping the periodic length fixed and increasing the fractional width of the iris sections. A second option involves the use of a structure with a similar pass-band in which the beam interacts with the spatial first harmonic. Both configurations will have the effect of lowering the interaction impedance, and thus be capable of delivering comparable output powers but with reduced electric fields at the walls of the structure.

In the work reported here the overall efficiency was limited to about 16% but the system has not been optimized. It is possible that similar performance, but with greater efficiency, can be obtained using the techniques described in the previous paragraph or even with devices with a somewhat lower interaction impedance. In addition to the transit time isolation acting to isolate the input from the output the relatively large insertion impedance of the second stage serves to enhance the isolation of the input from the output. It should be noted that we have not measured the phase stability of this particular device. However, based on experience with earlier amplifiers and simulation code results, we believe that we are operating in an amplifier mode.

We also note that the modification of the electron distribution function in the interaction has been measured directly

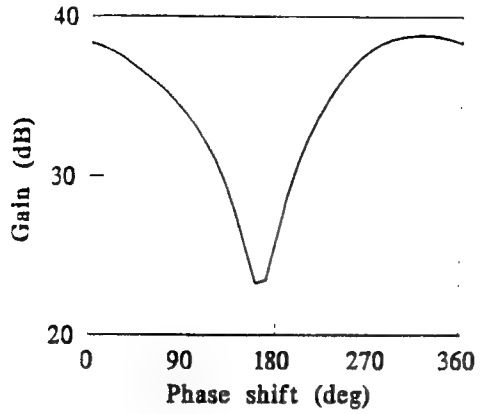

(a)

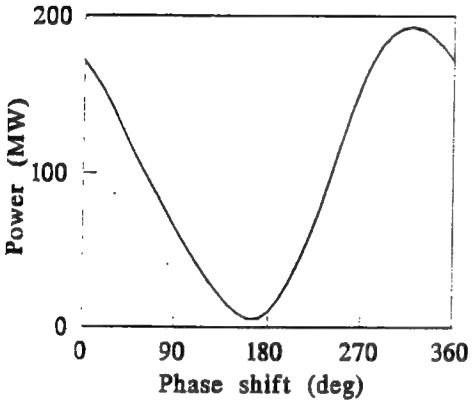

(b)

Fig. 8. Gain and output power in a two stage amplifier as a function of the phase shift between stages.

and is in good agreement with the predictions of codes. We believe that this is the first time that such measurements have been reported in high power TWT's. The existence of the high energy tail in the electron distribution was predicted by the simulation code and is evident when one considers that some of the electrons in the originally uniform beam were phased so that they would be preferentially accelerated. Even with the broad spread in the distribution function, gain still occurs as more particles loose energy to the rf wave than gain energy. It is interesting that the gain estimates, using Pierce theory, give reasonable results in view of this phenomenon.

In conclusion, we have developed a novel technique, transit time isolation, which may be used to eliminate sideband phenomena in high power TWT amplifiers. The experimental results are consistent with the main features of analytic and MAGIC code simulations of the amplifier.

ACKNOWLEDGMENT

The MAGIC simulation code was supplied by Mission Research Corporation.

REFERENCES

[1] L. Schächter, "New directions in RF sources," in *Proc. of the Particle Accelerator Conf.*, Washington, DC, May 17–20, 1993, to be published.
[2] E. Kuang, T. J. Davis, G. S. Kerslick, J. A. Nation, and L. Schächter, *Phys. Rev. Lett.*, vol. 71, p. 2666, 1993.
[3] D. Shiffler, J. A. Nation, and C. B. Wharton, *Appl. Phys. Lett.*, vol. 54, p. 674, 1989.
[4] D. Shiffler, J. A. Nation, and G. S. Kerslick, *IEEE Trans. Plasma Sci.*, vol. 18, p. 546, 1990.
[5] D. Shiffler, J. D. Ivers, G. S. Kerslick, J. A. Nation, and L. Schächter, *Appl. Phys. Lett.*, vol. 58, p. 899, 1991.
[6] D. Shiffler, J. A. Nation, J. D. Ivers, G. S. Kerslick, and L. Schächter, *J. Appl. Phys.*, vol. 70, p. 106, 1991.
[7] L. Schächter, J. A. Nation, and G. Kerslick, *J. Appl. Phys.*, vol. 68, p. 5874, 1990.
[8] L. Schächter, J. A. Nation, and D. Shiffler, *J. Appl. Phys.*, vol. 70, p. 114, 1991.
[9] L. Schächter, *Phys. Rev. A*, vol. 43, p. 3785, 1991.
[10] L. Schächter and J. A. Nation, *Phys. Rev. A*, vol. 45, p. 8820, 1992.
[11] L. Schächter and J. A. Nation, submitted to *J. Appl. Phys.*
[12] C. B. Wharton, L. M. Earley, and W. P. Ballard, *Rev. Sci. Instrum.*, vol. 57, p. 855, 1986.
[13] T. J. Davis, *Ph.D. Thesis*, Cornell University, 1993.
[14] Levi Schächter and John A. Nation, (submitted for publication in *Appl. Phys. Lett.*).

Erjia Kuang was born in Lei Yang, Hunan province, China on August 25, 1968. He received the B.S. degree in physics from Beijing University, Beijing, China, in 1989. He is now pursuing the Ph.D. degree in electrical engineering at Cornell in the field of high power microwave sources.

Timothy J. Davis, for a biography please see page 510 of this issue.

Jim Ivers worked as a metalographer at Sintercast Div. of Chromalloy Corp. for 2 years before going into the Navy in 1964. After four years working on aviation communications and navigation equipment, a student career at NJIT produced a B.S. in electrical engineering in 1972, during which he also participated in the development of the electromagnetic shock tube experiment at Columbia University.

Since 1972 he has been working with the Laboratory of Plasma Studies at Cornell University, building high voltage pulse machines and developing particle beam sources for use in particle accelerators and high power microwave amplifiers.

Graham S. Kerslick received a B.A. in physics and philosophy from the University of Lancaster, England, in 1977. He was awarded the Ph.D. in physics at Imperial College, London, in 1983.

He is a Research Associate with the Laboratory of Plasma Studies at Cornell University, Ithaca, NY. His current research activities include the study of electron beam sources and their application to the production of high power microwaves.

John A. Nation, for a biography please see page 510 of this issue.

Levi Schächter, for a biography please see page 510 of this issue.

High power microwaves at 9 GHz from an extended length cavity in a coaxial beam geometry

T. J. Davis, L. Schächter, and J. A. Nation
Laboratory of Plasma Studies and School of Electrical Engineering, Cornell University, Ithaca, New York 14853

(Received 29 March 1993; accepted for publication 15 July 1993)

Experiment and simulation demonstrate high power microwave generation at 9 GHz using a 9-cm-diam, 400-keV, 7-kA annular electron beam. The beam is propagated in a coaxial drift tube between inner and outer conductors, a configuration which increases the available beam current and reduces the surface fields from existing high power sources. The microwave interaction is provided by an extended length loaded cavity, overcoming the limitations of radiative loss and low quality factor usually imposed by the coaxial geometry. A coupler samples 25 MW of the total 200 MW produced by the beam-cavity interaction. Simulations indicate that the 7% efficiency can be significantly improved by optimizing the interaction length.

A number of high power microwave devices, such as relativistic klystrons,[1,2] gyroklystrons,[3] traveling wave tubes,[4] and free electron lasers[5] have emerged over the past years to converge on the radio frequency (rf) amplifier requirements for high gradient particle accelerator and high power radar applications. Common among these different approaches is the use of a high energy (>400 keV), high current (>100 A), short pulse ($\leqslant 2$ μs) electron beam to interact with resonant fields and structures in a single conductor waveguide, resulting in microwave power from several gigawatts to tens of megawatts at frequencies spanning the microwave spectrum from 1 to 30 GHz. As the devices are scaled to higher frequency or higher power, however, inherent problems remain due to the high field levels in the structures and the high gain of the interactions. Relativistic klystrons must use traveling wave output cavities, or rely on insulation at the cavity gaps, to avoid breakdown and pulse shortening. Gyroklystrons and traveling wave tubes must incorporate means to eliminate unwanted oscillations. In practice, the peak output power is limited in most devices by these considerations as well as the available beam power.

In this letter we report on a coaxial device which generates several hundred megawatts of single frequency radiation in X band. It is possible that a coaxial beam geometry can alleviate many limitations of existing sources. In this configuration, an annular beam is propagated between inner and outer drift tube conductors. Low power amplifiers[6] and high power oscillators[7] in a coaxial geometry have previously been reported. Recently, researchers have analyzed the coaxial Cerenkov interaction[8] and proposed use of a coaxial system to increase the limiting current in annular beam klystrons.[2] The advantage of a large average diameter coaxial configuration is twofold; it is capable of propagating very high currents in the annular beam, and the surface fields are reduced due to the increased volume in the microwave structures. Since the traverse magnetic (TM) mode cutoff frequencies are controlled only by the separation distance between conductors, single mode or discrete cavity interactions may still be preserved. The major disadvantage of a coaxial system is that the transverse electromagnetic (TEM) mode can propagate in the drift space. This transmission line mode will degrade the quality factor (Q) for standard, small-gap cavities from several thousand to less than a hundred, resulting in a profound loss of efficiency for a normal multicavity klystron arrangement.

To improve the interaction efficiency in our experiment, we designed and manufactured a 16-cm-long toroidal cavity lined with dielectric. Dielectrics were used for ease of analysis and manufacture, and can be replaced by metallic periodic structures for highest power operation. The extended cavity supports a TM_{01} mode at phase velocity $v_p < c$, thus providing a strong distributed interaction with the beam. The drift tube sections attached to the cavity are cutoff to the TM mode, indicating reflection at the cavity-drift tube boundaries. A substantial amount of cavity energy may be lost to the drift space TEM mode, however. The cavity is similar in many respects to a finite length traveling wave tube,[9] only that here we benefit from reflections and gain to actively increase the effective Q.

A schematic of the experiment is shown in Fig. 1. A conical cathode with a graphite tip is fully immersed in the uniform magnetic field of 1 T, and field emits a 2-mm-thick annular beam of 9-cm diameter. The beam parameters of 400 keV, 7 kA, and 50-ns duration are produced by an Experimental Test Accelerator transformer/Blumlein module.[10] The drift tube is composed of 7.6- and 9.8-cm-diam inner and outer conductors, and is terminated by a wedge-shaped silicon carbide absorber. Removing the ab-

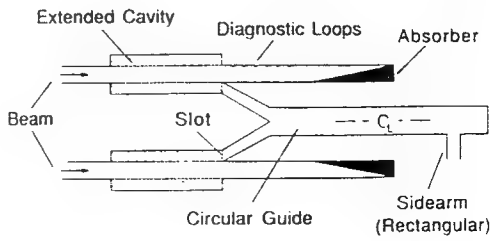

FIG. 1. Schematic of coaxial extended length cavity experiment. The experiment is ~1 m long with a maximum diameter of 12 cm. The slot (an aperture on the cavity endplate) and waveguide arrangement comprise the cavity coupler.

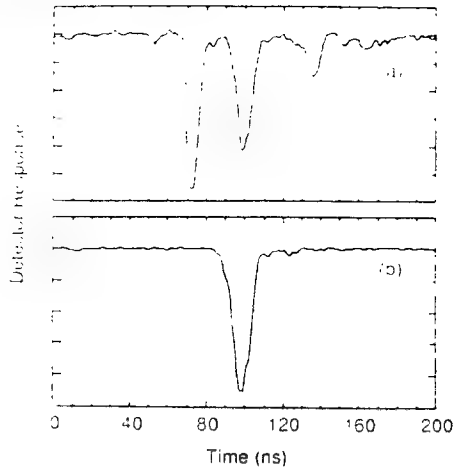

FIG. 2. Comparison of the dispersed signal from the cavity coupler without (a) and with (b) input power from the magnetron. The three peaks in (a) correspond to three separate frequencies; a single resonance (b) is selected at 9.1 GHz with input power in the range 10–30 kW.

sorber does not affect device operation. The cavity is loaded with 6-mm-thick acrylic liners on both the inner and outer surfaces. To diagnose the interaction, an azimuthal slot on the cavity endplate couples energy through a transition piece to circular waveguide. The 2.9-cm-diam circular guide TM_{01} mode is further converted to rectangular guide using a sidearm. This system (or cavity coupler) also serves as a means to input power from an external X-band magnetron to select the interaction frequency. Most of the cavity energy, however, is lost to the drift tube TEM mode, or ultimately to the absorber. Rf magnetic field probes, or pickup loops, placed downstream of the cavity thus provide additional information. Each diagnostic is monitored with a fast diode detector. Microwave emission typically occurs over 20–25 ns, centered around the period of peak beam power. Shorter wave forms (~ 10 ns) from the coupler are often observed, and indicate breakdown at the sidearm window. Fluctuations in the output signals across the pulse width are also common, and are likely due to the variations in beam voltage and current.

Two methods are used to identify the frequency of the output radiation. One is a long (~ 95 m) section of waveguide which acts as a dispersive line. We have improved the accuracy of this method to about 5 MHz using sensitive calibration and novel diagnostic techniques. An example wave form from the cavity coupler, dispersed using the long section of guide, is displayed in Fig. 2(a). Since the cavity operates on the beam over several wavelengths (~ 6), the microwave output without injected rf is distributed over several resonant modes. The three modes in Fig. 2(a) correspond in frequency to 9.6, 9.1, and 8.6 GHz. However, with input drive power from a magnetron at 9.1 GHz, the interaction is locked to the center resonance [see Fig. 2(b)]. The input power from the magnetron has been varied within the range 10–30 kW, although the exact levels have not been determined due to reflections in the coupling system. The coupler and loop signal amplitudes are insensitive to the magnitude of the external drive, and remain the same even in the absence of input power. Thus,

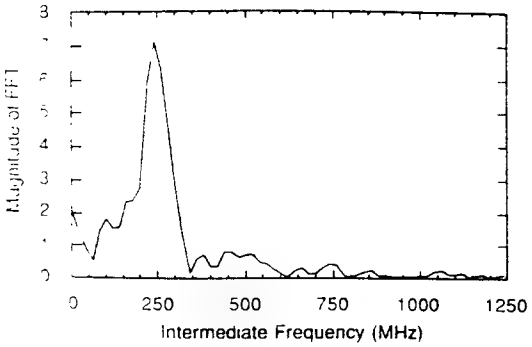

FIG. 3. FFT of mixer output from a magnetic field probe downstream of the cavity. The intermediate frequencies are obtained by mixing the loop signal with a local oscillator. The bandwidth of the radiation is less than 200 MHz.

the system operates as a single cavity oscillator. Using a double balanced mixer, we can obtain a second independent frequency measurement. A fast Fourier transform (FFT) of the mixed signal from a downstream magnetic field probe is shown in Fig. 3. With a local oscillator set above 9.3 GHz, and input drive power at 9.1 GHz, we obtain a dominant signal at the correct intermediate frequency. The bandwidth cannot be precisely determined from this technique because of the short microwave pulse duration, but is less than 200 MHz.

To provide an absolute measurement of the power flowing through the coupler, we have built and inserted a hot-air calorimeter[11] in place of the sidearm. Because of the mechanical design of the coupling system, the calorimeter has been used in the situations without external drive; regardless, the cavity oscillates to the same power level. In this arrangement, the calorimeter has measured up to a maximum of 25 MW of coupled power. A loop in the coupler tube samples the rf envelope, which has shown no evidence of breakdown in the absence of the sidearm window.

Using the 2 1/2 dimension particle-in-cell code MAGIC, we have performed simulations to model and verify the experimental results. A phase-space plot from the beam-cavity interaction is shown in Fig. 4. Although strong modulation and bunching is created through the cavity, electron reacceleration by the radiation field limits the efficiency of the interaction. This is a saturation mechanism characteristic of many high power microwave devices. Again, a single resonance of the cavity can be selected using input power through the simulation coupler. Figure 5 compares FFTs of the radial electric field in the coupler with and without 25 kW of input drive power. In single frequency operation, the output power flowing through the coupler is diagnosed to be 27 MW, in excellent agreement with the 25 MW from experiment. The total beam kinetic energy loss through the cavity is also measured to be about 200 MW, corresponding to an rf efficiency of 7%. We have performed other simulations to reduce the length of the cavity and avoid saturation effects, which result in total rf power of 500 MW for an increased efficiency of 18%.

To summarize, we have demonstrated that many of the

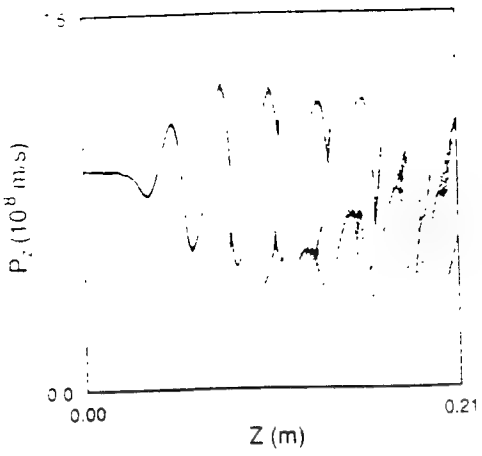

FIG. 4. Phase space of the simulation macroparticles, plotted as the normalized axial momentum $P_z=\gamma v$ (γ is the relativistic factor). Each macroparticle models approximately 10^9 beam electrons. Towards the end of the cavity, saturation reaccelerates the low energy particles, resulting in a loss of efficiency.

limitations of coaxial sources can be overcome using a single, extended length loaded cavity. We have sampled 25 MW of output power from a 16-cm-long cavity, corresponding to approximately 200 MW in the interaction region at 7% efficiency. The interaction may be locked to a single frequency with modest input power levels from an external X-band source. For the future, we have optimized the design to eliminate saturation effects, which in simulation have increased the total rf power to 500 MW at 18% efficiency. For more complete power extraction, sophisticated output coupler and converter designs are necessary.

This work was supported by the Department of Energy and the Air Force Office of Scientific Research. The MAGIC simulation code was supplied by Mission Research Corporation.

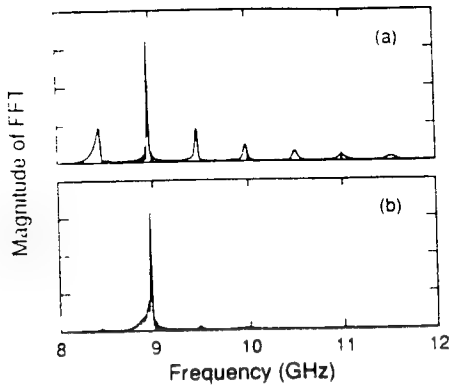

FIG. 5. Simulation FFTs of the radial electric field in the cavity coupler without input power to the cavity (a), and with 25 kW of input power (b). Without injected rf, the coupling occurs over numerous resonant frequencies, an indication of the low loss inherent in the simulation code.

[1] M. A. Allen *et al.* Phys. Rev. Lett. **63**, 2472 (1989).
[2] Y. Y. Lau, M. Friedman, J. Krall, and V. Serlin, IEEE Trans. Plasma Sci. **18**, 553 (1990).
[3] W. Lawson, J. P. Calame, B. P. Hogan, M. Skopec, C. D. Striffler, and V. L. Granatstein, IEEE Trans. Plasma Sci. **20**, 216 (1992).
[4] D. Shiffler, J. D. Ivers, G. S. Kerslick, J. A. Nation, and L. Schächter, Appl. Phys. Lett. **58**, 899 (1991).
[5] M. E. Conde and G. Bekefi, Phys. Rev. Lett. **67**, 3082 (1991).
[6] G. C. Dewey, P. Parzen, and T. J. Marchese, Proc. IRE **39**, 153 (1951).
[7] J. A. Nation, Appl. Phys. Lett. **17**, 491 (1970).
[8] E. P. Garate, A. Fisher, and W. T. Main, IEEE Trans. Plasma Sci. **18**, 831 (1990).
[9] L. Schächter, J. A. Nation, and G. Kerslick, J. Appl. Phys. **68**, 5874 (1990).
[10] R. E. Hester, D. G. Bubp, J. C. Clark, A. W. Chesterman, E. G. Cook, W. L. Dexter, T. J. Fessenden, L. L. Reginato, T. T. Yokota, and A. A. Faltens, IEEE Trans. Nucl. Sci. **NS-26**, 4180 (1979).
[11] C. B. Wharton, L. M. Earley, and W. P. Ballard, Rev. Sci. Instrum. **57**, 855 (1986).

Analytical method for studying a quasiperiodic disk loaded waveguide

Levi Schächter and John A. Nation
Laboratory of Plasma Studies and School of Electrical Engineering, Cornell University, Ithaca, New York 14853

(Received 3 June 1993; accepted for publication 20 August 1993)

An analytic method to investigate a quasiperiodic disk loaded waveguide is presented. We rely on Cauchy residue theorem to formulate the transmission and reflection from a system composed of radial arms and grooves provided that the inner radius is kept constant; all the other parameters of the system can be arbitrarily changed. This method was successfully utilized to design the input and output section of a high power traveling wave tube which is very sensitive to reflections from both ends. We found this method particularly useful for the design of the output regions where breakdown imposes constraints on the geometry.

In many high power devices the electromagnetic energy is confined and guided by metallic surfaces. These surfaces play an important role in the interaction process of the electrons with the electromagnetic wave(s). A klystron, for example, consists of a metallic pipe to which two or more cavities are connected. The pipe is designed such that at the frequency of interest the electromagnetic wave is below cutoff and in the absence of the beam the cavities are *isolated*. In this kind of structure, power levels of 50 MW at 11.4 GHz were achieved at SLAC,[1] but since the interaction occurs in the close vicinity of the cavity gap, the gradients at the output cavity are high and the system is susceptible to rf breakdown.

This problem is less severe in a disk loaded traveling wave tube (TWT) which consists of a series of *coupled* cavities. These cavities are basically a short section of a periodic structure. In this case the interaction is no longer confined to the vicinity of the cavity, but it is distributed along the entire structure. The first experiments on high power TWT performed at Cornell[2] indicated that 100 MW at 8.76 GHz can be achieved before the system oscillates. Although no rf breakdown was observed in these kind of structures the fact that the input is no longer isolated from the output allows waves to be reflected backwards and this feedback may ultimately cause the system to oscillate.

In order to isolate the input from the output, the TWT was split in two sections separated by a sever.[3] The second set of experiments on two stage high power TWT indicated that power levels in excess of 400 MW are achievable with no indication of rf breakdown.[3] In this case, however, the output spectrum was 300-MHz wide and a significant amount of power (up to 50%) was measured in asymmetric sidebands. The latter observation was investigated theoretically[4] and it was concluded that it is a result of amplified noise at frequencies selected by the interference of the two waves bouncing between the ends of the last stage. In fact we have shown[5] that what we call amplifier and oscillator are the two extremes of possible operation and any practical device operates somewhere in between according to the degree of control we have on the reflection process. We have suggested[6] a method to eliminate the problem of reflections by designing a structure in which the time it takes the first reflection to reach the input end is of the same order of magnitude as the electron pulse length, thus by the time the reflection becomes relevant there are no more electrons to interact with. This method was successfully demonstrated[7] experimentally and power levels of 200 MW were achieved at 9 GHz. The spectrum of the output signal was less than 50 MHz and the passband of the periodic structure is less than 200 MHz—for this reason we call it the narrow band structure (NBS). The 200 MW power levels, generated with the NBS were accompanied by gradients larger than 200 MV/m. Although we did not experience rf breakdown for any further increase in the power levels it will be necessary to increase the volume of the last two or three cells in order to minimize the electric field on the metallic surface—thus the system becomes quasiperiodic.

To summarize, the main two problems of an extraction section based on a quasiperiodic disk loaded structure are (1) minimize the reflections at both ends of the structure in order to avoid oscillation at high power levels and (2) taper the output section in order to avoid breakdown and optionally compensate for the velocity decrease of the electrons. In order to optimize these two conflicting requirements we have developed an analytical technique which permits us to design a quasiperiodic structure. This is a model which takes into account the input region, a section of a uniform structure, and the output region. In this letter we shall discuss only the pure electromagnetic problem and the analysis of an active device is left for an extended article. Although we are highly motivated here by the high

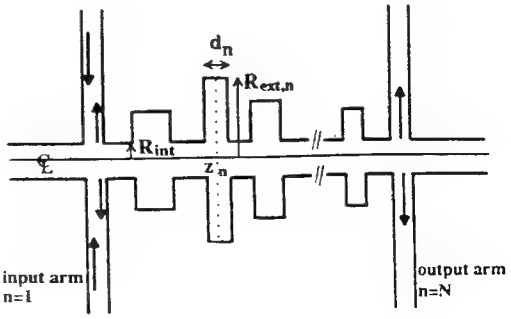

FIG. 1. The schematic of the system under consideration. The external radius R_{ext}, the groove/arm width d, and the separation between any two cavities can be arbitrary. The internal radius R_{int} has to be maintained the same. z_n indicates the center of the groove/arm.

 0003-6951/93/63(17)/2441/3/$6.00

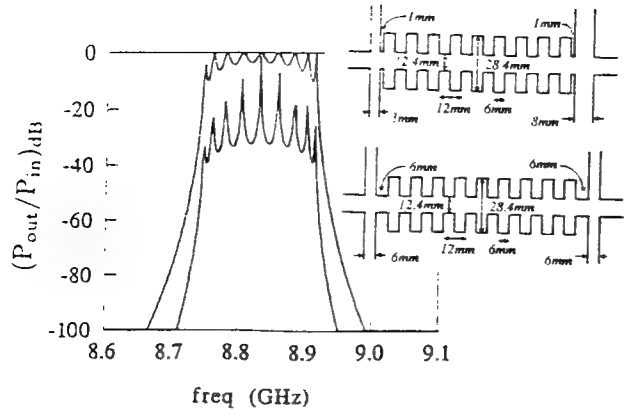

FIG. 2. The effect of the separation of the input and output arm from the cavity. The lower transmission curve corresponds to the 6 mm case.

power TWT system, our analysis applies to klystrons,[8] backward oscillators, multimode Cerenkov devices and, with adequate variations, it can take into account the effect of extraction cells in magnetrons.

In this analysis we shall consider only TM_{01} mode. The only constraint of the method is that the radius of the pipe (R_{int}) has to be kept constant along the entire system. The schematics of the latter is presented in Fig. 1. It consists of a radial input arm of width d_1, a number of cells which is limited only by the computational capabilities and an output arm of a width d_N where N is the total number of cells and arms. It is also possible to extend the analysis to include more than one output arm.[8]

Unlike in a periodic structure where the field in the inner cylinder ($0<r<R_{int}$) can be represented by Floquet series, here we have to consider the entire spatial spectrum of waves, therefore the magnetic vector potential reads

$$A_z(r,z;\omega)=\int_{-\infty}^{\infty} dk\, A(k) I_0(\Gamma r) e^{-jkz}, \tag{1}$$

where $\Gamma^2=k^2-\omega^2/c^2$, $I_0(x)$ is the modified Bessel function of the first kind and the system is assumed to be in steady state ($e^{j\omega t}$). In the arms or grooves the electromagnetic field can be represented by a superposition of modes which satisfy the boundary conditions on the metallic walls. In principle an infinite number of such modes should be taken. Our experience indicates that as long as the vacuum wavelength is about 5 times larger than the groove/arm width the first mode [transverse electric magnetic (TEM)] is sufficient for most practical purposes. This assumption is by no means critical for the present analysis and the arguments are very similar when a larger number of modes is required, however we use it since it makes the presentation much simpler. Within the framework of this approximation we can write for the magnetic vector potential in the input arm

$$A_z(r,z;\omega)=A_{in}H_0^{(1)}\left(\frac{\omega}{c}r\right)+D_1H_0^{(2)}\left(\frac{\omega}{c}r\right), \tag{2}$$

where $H_0^{(1)}(x)$ and $H_0^{(2)}(x)$ are the zero-order Hankel function of the first and second kind, respectively; A_{in} represents the amplitude of the incoming wave, and D_1 is the

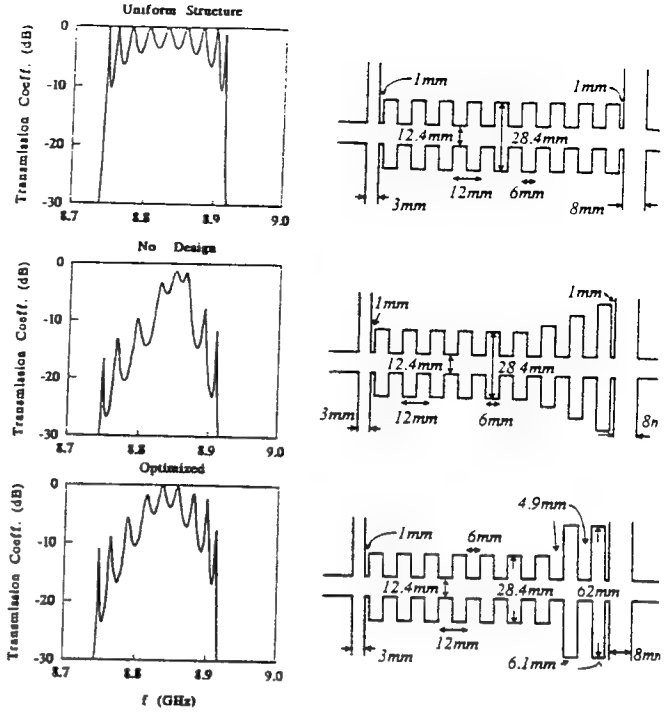

FIG. 3. Design of a structure subject to the constraint of increasing th volume of the last cells dictated by the breakdown considerations. Th linear (adiabatic) taper is not adequate in short and high power systems When the output cavities have one frequency which is close to that of th cavities in the uniform structure the system can be readily tuned.

amplitude of the reflected wave which is yet to be determined. In the nth ($1<n<N$) groove we have

$$A_z^n(r,z;\omega)=D_nT_{0,n}\left(\frac{\omega}{c}r\right), \tag{3}$$

D_n is the amplitude of the magnetic vector potential, $T_{0,n}(\omega/cr) = J_0[(\omega/c)r]Y_0[(\omega/c)R_{ext,n}] - Y_0[(\omega/c)r]J_0[(\omega/c)R_{ext,n}]$, and $R_{ext,n}$ is the external radius of the nth groove; later we shall also use the function $T_{1,n}[(\omega/c)r] = J_1[(\omega/c)r]Y_0[(\omega/c)R_{ext,n}] - Y_1[(\omega/c)r]J_0[(\omega/c)R_{ext,n}]$.

$J_\nu(x)$ and $Y_\nu(x)$ are the ν order Bessel function of the first and second kind, respectively. Finally in the output arm

$$A_z(r,z;\omega)=D_NH_0^{(2)}\left(\frac{\omega}{c}r\right). \tag{4}$$

In order to determine the various amplitudes we next impose the boundary conditions in a way which is similar to what is being done in the case of a periodic structure. The main difference is that we no longer can look at one cell to characterize the entire system but we have to consider each individual region.

It is convenient to represent the entire electromagnetic problem in terms of the amplitudes of the mode in the grooves and arms, i.e.,

$$\sum_{m=1}^{N}\tau_{n,m}D_m=S_nA_{in}, \tag{5}$$

where, $\tau_{n,m}=\psi_{1,n}\delta_{n,m}-\psi_{0,m}\chi_{n,m}$, $S_n=-H_1^{(1)}(\alpha)\delta_{n,1}+H_0^{(1)}(\alpha)\chi_{n,1}$ and

$$\chi_{n,m}=\frac{d_m\alpha}{2\pi}\int_{-\infty}^{\infty}dk\,\frac{I_1(\Delta)}{\Delta I_0(\Delta)}\,L_n^*(k)\,L_m(k). \tag{6}$$

In these expressions $\delta_{n,m}$ represents the Kroniker delta function and the asterisk represents the complex conjugate. In addition,

$$\alpha=\frac{\omega}{c}R_{\rm int},\quad \Delta=\Gamma R_{\rm int},\quad L_n(k)=\frac{1}{d_n}\int_{z_n-d_n/2}^{z_n+d_n/2}dz\,e^{jkz} \tag{7}$$

and

$$\psi_{\nu,n}=\begin{cases}H_\nu^{(2)}(\alpha), & n=1 \text{ or } n=N\\ T_{\nu,n}(\alpha), & 1<n<N\end{cases} \tag{8}$$

with $\nu=0,1$; z_n is the location of the center of the nth groove or arm and d_n is the corresponding width.

The next step is to evaluate the integral which defines the matrix χ in terms of analytic functions. This is done by using the Cauchy residue theorem. First we substitute the explicit expressions for $L_n(k)$ from Eq. (7); the result is

$$\chi_{n,m}=\frac{d_m\alpha}{2\pi}\frac{1}{d_m}\int_{z_m-d_m/2}^{z_m+d_m/2}dx_1\frac{1}{d_n}\int_{z_n-d_n/2}^{z_n+d_n/2}dx_2 \times\int_{-\infty}^{\infty}dk\,\frac{I_1(\Delta)}{\Delta I_0(\Delta)}\,e^{jk(x_1-x_2)}. \tag{9}$$

If we now examine the integrand we observe that there are an infinite set of poles which correspond to $I_0(\Delta)=0$. Bearing in mind the relation between the modified Bessel function and the regular one $[J_0(x)]$ we realize that the condition above is satisfied for $k^2=(\omega/c)^2-(p_s^2/R_{\rm int}^2)$; here p_s are all the zeros of the zero-order Bessel function of the first kind, i.e., $J_0(p_s)\equiv 0$. According to the Cauchy's theorem the contribution to the integral will come from the poles of the integrand; hence the last integral in Eq. (9) reads

$$\frac{1}{2\pi}\int_{-\infty}^{\infty}dk\,\frac{I_1(\Delta)}{\Delta I_0(\Delta)}\,e^{jk(x_1-x_2)} =\frac{1}{\pi R_{\rm int}^2}\sum_{s=1}^{\infty}\int_{-\infty}^{\infty}dk\,\frac{e^{jk(x_1-x_2)}}{k^2+\Gamma_s^2}, \tag{10}$$

where $\Gamma_s^2=(p_s/R_{\rm int})^2-(\omega/c)^2$. The last integral is the Green function of a uniform waveguide and is easily evaluated as $G(x_1|x_2)=(\pi/\Gamma_s)e^{-\Gamma_s|x_1-x_2|}$. This result permits us to express the matrix χ in terms of analytic functions since the integration on x_1 and x_2 in Eq. (9) is straightforward; the result is

$$\chi_{n,m}=\frac{\alpha}{R_{\rm int}^2}\sum_{s=1}^{\infty}\begin{cases}\dfrac{2}{\Gamma_s^2}\left[1-e^{-\Gamma_s d_n/2}\,\mathrm{sinhc}(\Gamma_s d_n/2)\right], & n=m\\ \dfrac{d_m}{\Gamma_s}e^{-\Gamma_s|z_n-z_m|}\,\mathrm{sinhc}(\Gamma_s d_n/2) \times\mathrm{sinhc}(\Gamma_s d_m/2), & \text{otherwise}\end{cases} \tag{11}$$

In this expression $\mathrm{sinhc}(x)=\sinh(x)/x$. The electromagnetic problem has been now simplified to inversion of a matrix whose components are analytic functions. The transmission pattern of the structure fits well the predictions of the dispersion relation of an infinite structure.

Next we shall illustrate the potential of this method. And the first goal is to determine what should be the location of the arms to adequately feed power into a nine cell narrow band structure ($R_{\rm ext}=14.2$ mm, $R_{\rm int}=6.2$ mm, cell length $L=12$ mm half of which is the groove). Figure 2 illustrates the geometry of the NBS with nine cavities and two arms. In the first case the arms are 6 mm from the first cells and we observe that the average transmission coefficient is -20 dB. When the drift region was shortened to 1 mm the transmission coefficient increases dramatically to an average value of -3 dB (this result was qualitatively observed in experiment). Let us now assume for a moment that we have matched the cold system for a given frequency, i.e., the gain in dB, $10\log(|D_N|^2 d_N/|A_{\rm in}|^2 d_1)$ is zero. We know that in the NBS very high gradients develop in the interaction process—in particular in the last couple of cells. In order to avoid rf breakdown, we want to increase the volume where the electromagnetic energy is stored and by that we lower the energy density and consequently the field. We started with a linear tapering of the external radius of the last three cells. The width of these cells and their separation was varied in a wide range of parameters to bring the transmission coefficient to 0 dB at a given frequency and the best we could achieve was -3 dB which is not acceptable; see Fig. 3. At this stage we returned to the initial geometry but doubled the external radius of the last two cells. These cavities have two (rather than one) resonant frequencies, one of which is close to that of a cavity in the uniform structure. After some fine tuning we obtained the transmission which is optimized to the required frequency.

In conclusion, we have presented a method to calculate the electromagnetic characteristics of a quasiperiodic structure which consists of radial arms and a set of coupled disk loaded cells. The only constraint in this method is that the internal radius has to be kept constant. We have used it already to investigate the beam-wave interaction in transition region. The results will be presented in an extended version of this work.

This work was supported by the United States Department of Energy and AFOSR.

[1] G. A. Loew, in HEACC'92, XVth International Conference on High Energy Accelerators, Hamburg, Germany, 20–24 July 1992 (World Scientific, River Edge, NJ, 1992), p. 777.
[2] D. A. Shiffler, J. A. Nation, J. D. Ivers, G. S. Kerslick, and L. Schächter, Appl. Phys. Lett. **58**, 899 (1991).
[3] D. A. Shiffler, J. A. Nation, J. D. Ivers, G. S. Kerslick, and L. Schächter, J. Appl. Phys. **70**, 106 (1991).
[4] L. Schächter, J. A. Nation, and D. A. Shiffler, J. Appl. Phys. **70**, 114 (1991).
[5] L. Schächter and J. A. Nation, Phys. Rev. A **45**, 8820 (1992).
[6] L. Schächter and J. A. Nation, AIP Conf. Proc. **279**, 56 (1992).
[7] E. Kuang, T. J. Davis, G. S. Kerslick, J. A. Nation, and L. Schachter (unpublished).
[8] M. A. Allen, Phys. Rev. Lett. **63**, 2472 (1989).

Transit Time Isolation of a High Power Microwave Amplifier

E. Kuang, T. J. Davis, G. Kerslick, J. A. Nation, and L. Schächter
Laboratory of Plasma Studies and School of Electrical Engineering, Cornell University, Ithaca, New York 14853
(Received 2 June 1993)

We report experimental results from a high power X-band traveling wave tube amplifier designed to eliminate sidebands due to reflections from its output. The amplifier has a very low energy velocity, such that the time it takes a wave to be reflected from the output to the input is of the order of, or greater than, the electron beam pulse duration. The bandwidth of the output spectrum is limited by the very narrow passband of the periodic structure. The amplifier has been operated at power levels of up to 160 MW at 9 GHz for pulse durations of 50 ns.

PACS numbers: 85.10.Jz, 41.75.Ht

The high power microwave requirements of the next linear collider (NLC) are very demanding, typically of order 200 MW per meter of acceleration structure. This is expected to correspond to a gradient of 100 MV/m for a pulse duration of more than 100 ns. The general trend in this area of research [1] is to expand beyond the S-band klystron to frequencies in the range 10–35 GHz. The main reason for this trend is that for a given accelerating gradient the necessary microwave power varies qualitatively as the inverse of the operating frequency squared ($P \propto f^{-2}$). Thus an increase by a factor of 3 in the frequency can lower the necessary power by 1 order of magnitude. This increase in the frequency is accompanied by a corresponding reduction in the physical dimensions of the klystron's cavities and drifting region. This becomes a significant drawback when rf breakdown is considered. The smaller the volume of the cavity, for a given stored energy, the larger the electric fields and thus the probability of rf breakdown increases. This problem becomes acute in the extraction cavity.

In order to overcome this problem it is possible to replace the extraction cavity by a traveling wave structure, i.e., a disk loaded waveguide. Unlike the klystron where the cavities are electromagnetically isolated (by the drift region which is below cutoff) the traveling wave structure is a set of coupled cavities. In this case the beam-wave interaction is distributed along the entire interaction length whereas in a klystron it is limited to the close vicinity of the cavity.

The use of traveling wave amplifiers for the production of high power microwave radiation in the X band has been reported previously [2–5]. In a single stage amplifier, which consists of a section of corrugated waveguide, driven by a 0.85 MV, 0.8–1.6 kA, 100 ns electron beam, total power levels of up to 150 MW were measured. Beyond these power levels the system was noisy and prone to oscillation. In addition, for output powers above 80 MW the output spectrum showed the development of sidebands.

The coupling between the cavities also permits a backward electromagnetic wave to propagate. At very high gain this wave may cause the system to oscillate. To avoid the single stage oscillations, which are caused by the reflection of an electromagnetic wave from the output end of the amplifier to its input, a two-stage severed amplifier was developed. This device consists of two rippled wall waveguides isolated from each other by a sever, consisting of a lossy section of waveguide operated below cutoff. The space charge waves, which develop along the beam in the first stage, propagate through the sever whereas the electromagnetic mode is strongly (−25 dB) attenuated. In addition, the sever attenuates the reflected wave from the output end of the second stage, and prevents system oscillation due to feedback. With this device total power levels of up to 400 MW were achieved for beam currents of 0.8–1.2 kA and with an efficiency of more than 40%. Sidebands were observed at all output power levels in the two-stage amplifier, with the output spectrum extending over 300 MHz. The sidebands were asymmetrically located with respect to the input frequency and at the highest output levels carried up to 50% of the power.

In parallel with these experiments, theoretical analysis [6–9] has shown several interesting results: (i) As a result of the interaction process the energy spread of *individual* electrons can be as high as 60% of the initial beam energy, while the *average* energy of the beam is reduced by less than 10% [6]. (ii) When end effects are included the pure electromagnetic transmission characteristics of a slow wave structure are dominated by reflections which cause a frequency dependent standing wave pattern. This results in waves of certain frequencies being preferentially transmitted, whereas others are partially reflected. The separation of the transmission peaks, Δf, is determined by the total length of the structure d and the group velocity (V_{gr}) by the relation $\Delta f = V_{gr}/2d$. In the presence of an electron beam the peak value of the transmission coefficient increases due to the gain but the separation of discrete peaks remains unchanged. Consequently, the effective bandwidth of the interaction becomes narrower

0031-9007/93/71(16)/2666(4)$06.00

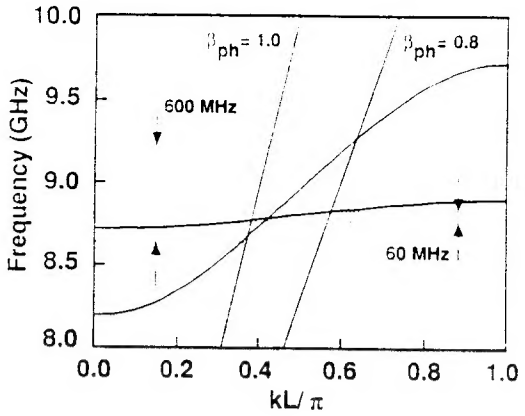

FIG. 1. Dispersion relations for a broad band and for a narrow band periodic structure, illustrating the decrease in bandwidth of an amplified signal in a low group velocity structure.

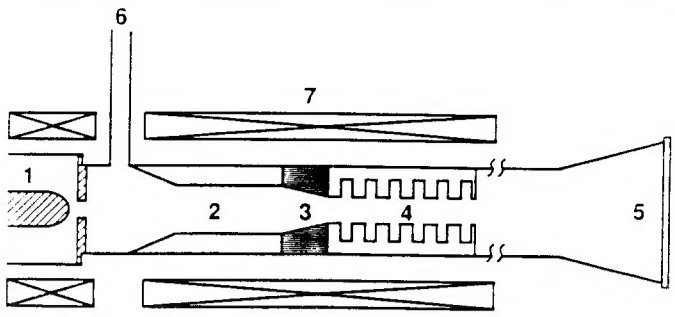

FIG. 2. Schematic showing the assembly of a two-stage severed amplifier. The first stage uses a dielectric loaded amplifier and the second stage a 10 period narrow band (low group velocity) structure. (1) Electron beam diode, (2) dielectric first stage, (3) silicon carbide sever, (4) narrow band structure, (5) output horn, (6) input waveguide, (7) magnetic field coils.

by the gain factor [7]. (iii) The ideal picture of an amplifier is a device in which the wave amplitude grows in space but remains constant in time, whereas in an ideal oscillator the amplitude grows in time but is constant in space. Any practical device operates somewhere between these two limiting cases [8].

Based on these studies we developed a qualitative model which explains the presence of the asymmetric sidebands. The essence of the model is as follows. The electrons are bunched by the wave and, depending on their phase relative to that of the wave, are either accelerated or decelerated. In this process they acquire a broad range of velocities. As they traverse the periodic structure the electrons generate spontaneous radiation in a frequency range which is directly related to their velocity spread: $\delta\omega/\omega \approx \frac{\delta V}{V_0}/(1-V_0/V_{gr})$ where V_0 is the average velocity of the electrons. The electromagnetic output spectrum is determined by the frequency selection due to the reflections and the subsequent amplification of the radiation by the beam. The selected frequencies correspond to the peaks in the transmission coefficient and thus the amplified noise is revealed as asymmetric sidebands, since the transmission peaks are determined primarily by the geometry, and not by the input frequency.

Since an output spectrum wider than 100 MHz is not acceptable for most applications of interest, we designed [9] an amplifier to eliminate the unwanted reflections. In a 15 cm long amplifier with a structure group velocity of $V_{gr} = 0.007c$, it takes about 75 ns for a reflected wave to reach the input. This is approximately equal to the electron pulse duration, and consequently the beam is unaffected by the time the reflected wave amplitude becomes significant at the input to the amplifier. An equivalent interpretation relies on the dispersion relation of two periodic structures; see Fig. 1. If the passband is 1.7 GHz, as in the original amplifier [2,3], an electron velocity spread between $0.8c$ and $1.0c$ can generate noise in a 600 MHz frequency range, whereas in the narrow passband (200 MHz) structure described here, the noise generated restricts the coherent signal to a width of 60 MHz. Transit time isolation in free electron lasers has been used previously to isolate the diagnostics from the input signal [10]. In the remainder of this Letter we report experimental results which show that the transit time isolation design eliminates sideband development.

Figure 2 shows a schematic of the experiment. The first stage is a medium power Cherenkov amplifier [9] which consists of a 1.6 cm radius waveguide partially loaded with STYCAST HIK dielectric material ($\epsilon = 5.0$). It is 30 cm long including a 5 cm taper at the input, and is followed by a 15 cm silicon carbide sever. The narrow band amplifier serves as the second stage of the system and consists of a ten period iris loaded waveguide. The structure has a 1.2 cm period, and a 1.42 cm external radius. Each iris is 0.6 cm long with an internal radius of 0.62 cm. To couple the power out of the narrow band structure, the length of the last iris is reduced to 0.1 cm. This modification is essential for efficient output coupling. The system is driven by a 1 MV, 1 kA, 50 ns, 0.6 cm diam electron beam. The microwave input signal is provided by an X-band magnetron which injects $\sim$ 30 kW into the dielectric first stage. The output power of this single stage alone is of order 3–5 MW, and has been increased to 50 MW before rf breakdown occurs on the dielectric. The main reason for the use of this Cherenkov amplifier was to prebunch the beam, and as a simple method to control reflections from the ends of the first stage.

The output power of the two-stage amplifier is determined using far field measurements of the gain. Figure 3 shows this power as a function of input frequency. Power levels from independent calorimetric measurements [11,12] correlate well with the gain data up to 65 MW. Above this level the pressure transducer in the calorimeter saturated. Output powers of 160 MW at 8.9 GHz have been measured for the full 50 ns electron

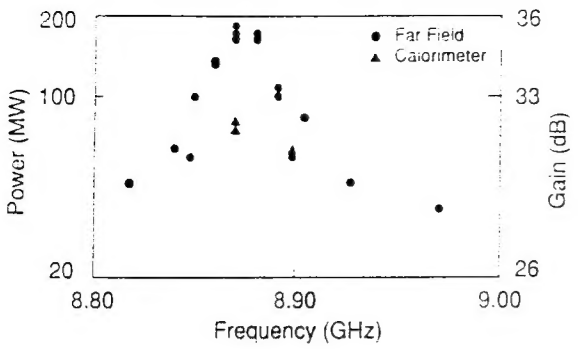

FIG. 3. Measured frequency response of the two-stage amplifier. The triangles indicate calorimetric data and the circles data obtained from the far field measurements. The calorimeter output saturates at about 65 MW.

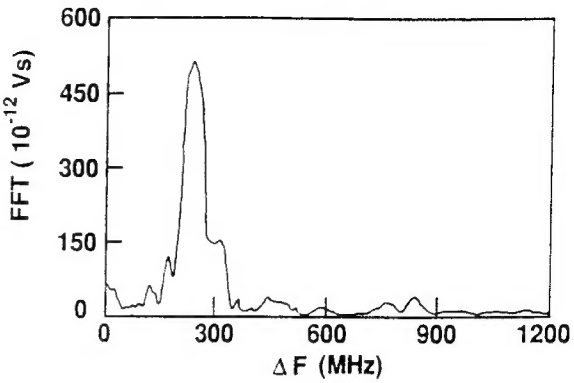

FIG. 4. Fast Fourier transform of the measured output signal from the two-stage amplifier showing the single frequency output.

beam duration. Pulse shortening has been observed at higher power levels of ~180 MW. This may indicate the onset of rf breakdown problems. The frequency content of the sampled output signal is measured with a double balanced mixer using heterodyning techniques. A typical fast Fourier transform (FFT) is illustrated in Fig. 4. The signal is at the input frequency and has a width of 48 MHz. The 50 ns pulse width of the output signal introduces a minimum FFT width of 20 MHz and will produce side lobes in the transform. If we interpret the secondary peaks of the FFT at 9 GHz as sidebands, a worst case scenario, then the sideband level has been reduced by at least 10 dB compared to that achieved in our earlier work [4].

The interaction in the narrow band structure has been studied both analytically and with the particle-in-cell code MAGIC. The analytical results indicate that a gain of 5–7 dB/cm can be expected compared to 1–2 dB/cm in the broad passband structure. This results from the high impedance ($Z \sim 1/V_{gr}$) of such narrow bandwidth amplifiers which, in turn, leads to high values of electric field in the structure. Calculations show that for output powers of 200 MW the electric field on the wall will be 200 MV/m. In order to reduce the interaction impedance and hence the electric stress on the walls a number of options may be available. The design can be modified to maintain the bandwidth, but increase the radius of the iris sections. Alternatively, operation at the first spatial harmonic of the structure may also be considered.

The sever section plays a crucial role in determining the output power level by introducing a change in the phase angle between the current density modulation and the longitudinal E field compared to that in the traveling wave tube section. Our 1D code indicates that the output power may range from 190 MW down to a few MW as the phase shift changes from 300° to 150° at the input to the narrow band structure.

Numerical simulations using the MAGIC code confirm that the sidebands have been essentially eliminated through the use of narrow band structures. The high gain feature within the passband is also confirmed, with the output power level dropping to ~ 6 MW outside the passband. At present we are unable to model the details of the sever within the particle-in-cell code and cannot make a detailed numerical comparison with our experimental results. Further work is in progress to adequately model the sever to include, not only the electromagnetic isolation of the input from the output, but also its influence on the space charge modes.

In conclusion, we have developed a novel technique, transit time isolation, which may be used to eliminate sideband phenomena in high power traveling wave amplifiers. This method may be extended to longer pulse durations than those reported here, but is clearly not appropriate where microsecond pulses may be required. The experimental results are consistent with the main features of analytic and MAGIC code simulations of the amplifier.

This work was supported by the Department of Energy and the Air Force Office of Scientific Research. The MAGIC simulation code was supplied by Mission Research Corporation.

[1] L. Schächter, in Proceedings of the Particle Accelerator Conference, Washington DC, 17–20 May 1993 (to be published).
[2] D. Shiffler, J. A. Nation, and C. B. Wharton, Appl. Phys. Lett. **54**, 674 (1989).
[3] D. Shiffler, J. A. Nation, and G. S. Kerslick, IEEE Trans. Plasma Sci. **18**, 546 (1990).
[4] D. Shiffler, J. A. Nation, J. D. Ivers, G. S. Kerslick, and L. Schächter, J. Appl. Phys. **70**, 106 (1991).
[5] D. Shiffler, J. D. Ivers, G. S. Kerslick, J. A. Nation, and L. Schächter, Appl. Phys. Lett. **58**, 899 (1991).
[6] L. Schächter, J. A. Nation, and G. Kerslick, J. Appl. Phys. **68**, 5874 (1990).
[7] L. Schächter, J. A. Nation, and D. Shiffler, J. Appl. Phys.

70, 114 (1991).
[8] Levi Schächter and J. A. Nation, Phys. Rev. A 45, 8820 (1992).
[9] Levi Schächter and J. A. Nation, in Proceedings of the Workshop on Advanced Acceleration Concepts, Port Jefferson, June 1992 (to be published).
[10] T. J. Orzechowski, B. Anderson, W. M. Fawley, D. Prosnitz, E. T. Scharlemann, S. Yarema, D. Hopkins, A. C. Paul, A. M. Sessler, and J. Wurtele, Phys. Rev. Lett. 54, 89 (1985).
[11] E. Garate, H. Kosai, K. Evans, and A. Fisher, Appl. Phys. Lett. 56, 1092 (1990).
[12] C. B. Wharton, L. M. Earley, and W. P. Ballard, Rev. Sci. Instrum. 57, 855 (1986).